36-year study reveals the effects of microhabitats on a wild wheat population

Tal Dahan-Meir[1], Thomas James Ellis[2], Fabrizio Mafessoni[1], Hanan Sela[3,4], Ori Rudich[1], Jacob Manisterski[4], Naomi Avivi-Ragolsky[1], Amir Raz[1,5], Moshe Feldman[1], Yehoshua Anikster[4], Magnus Nordborg[2*], Avraham A. Levy[1*]

[1]Department of Plant and Environmental Sciences, Weizmann Institute of Science; Rehovot, Israel.

[2]Gregor Mendel Institute, Austrian Academy of Sciences, Vienna BioCenter; Vienna, Austria.

[3]Institute of Evolution, University of Haifa; Haifa, Israel.

[4]The Institute for Cereal Crops Improvement, Tel-Aviv University; Tel Aviv, Israel.

[5]Migal, Galilee Technology Center; Kiryat Shmona, Israel.

*Corresponding authors: Avraham A. Levy, Magnus Nordborg.

Emails: avi.levy@weizmann.ac.il; magnus.nordborg@gmi.oeaw.ac.at

Abstract

Long-term genetic studies of wild populations are very scarce but are essential for connecting ecological and population genetics models, and are also necessary for understanding how climate change can affect biodiversity. We present a study of the wild ancestor of modern wheat, carried out over a 36-year period during which atmospheric CO_2 increased by 70 ppm and temperature by 1.5^{o}C. We genotyped 832 individuals from regular sampling along transects during the course of the experiment. Genotypes were clustered into ecological microhabitats over scales of tens of meters, and this clustering was remarkably stable over the 36 generations of the study. Simulations indicate that neutral processes alone are insufficient to explain this spatial and temporal stability, suggesting a role for fine-scale local adaptation to ecological parameters. Using a common-garden experiment, we showed that the genotypes found in distinct microhabitats differ phenotypically, further supporting the hypothesis of local adaptation. Our results provide a rare insight into the dynamics of a natural population at the scale of individuals over a period of environmental change.

Introduction

Climate change is a looming threat to plant biodiversity and food security (Hoffmann and Sgró, 2011; Pecl et al., 2017; Urban, 2015). This increases the importance of wild progenitors of crops because their genetic diversity is an immense reservoir of biotic and abiotic stress-resistance genes (Khoury et al., 2021). Sustained studies of progenitor species in their natural ecological niches can provide a better understanding of the likely impacts of climate change, and inform strategies for conservation of such resources *in-situ* as well as in gene banks (Wintle et al., 2019).

We examined the genetic diversity of a population of wild emmer wheat (*Triticum turgidum ssp. dicoccoides*) in Ammiad, Israel, which has been monitored for 36 years (Figure 1A). The original motivation for studying this particular population long-term was its high genetic diversity compared to other wild wheat populations (Felsenburg et al., 1991; Levy and Feldman, 1988), together with variable topography (Figure 1A, Movie S1) and a diversity of ecological niches. These parameters were ideal for investigating adaptation to microhabitats and to analyze the dynamics of the population over time in order to assess strategies for *in-situ* conservation. When the experiment started in 1984, climate change was not yet an established fact. In retrospect, the increase in local ambient temperatures by ~1.5 degrees Celsius (Figure 1B) and in atmospheric CO_2 concentration by 70 ppm (Figure 1C) (Keeling et al., 2001) during the course of the experiment, enabled us also to assess the effect of climate change on the genetic makeup of the population. For example, we could test if the overall genetic variation of the population or the spatial distribution of genotypes had changed. The study was also motivated by the fact that wild emmer wheat biodiversity is an invaluable resource for food security. Wild emmer wheat, a self-pollinating,

allotetraploid annual cereal (genome BBAA), is the progenitor of durum wheat (*T. turgidum ssp. durum*) and the maternal donor of the A and B sub-genomes of bread wheat (*T. aestivum*, genome BBAADD)(Levy and Feldman, 2022), and any gene from wild emmer wheat can be easily transferred to the background of domesticated wheat. Dense population transects were regularly sampled nine times between 1984 and 2020, and each plant was genotyped by sequencing. Earlier spatio-temporal studies of wild plants involved shorter periods, as well as less comprehensive or lower resolution sampling (Franks et al., 2007; Fu et al., 2019; Horovitz and Feldman, 1991; Kolis et al., 2022; Ozbek et al., 2007; Todesco et al., 2020; Volis et al., 2004). Indeed, long-term studies of species in their natural habitat are exceedingly rare. In animals, Soay sheep and Florida scrub-jays have been studied for periods ranging between 23 to 36 years (Aguillon et al., 2017; Ashraf et al., 2021; Chen et al., 2019; Stoffel et al., 2021), comparable to our study in years (but not generations). In plants, detailed studies of population structure did not cover more than eight years, and most did not involve consecutive samplings (Frachon et al., 2017; Hendrick et al., 2016; Kolis et al., 2022). Without such studies, it is difficult to connect abstract population genetics models of allele-frequency change with real-world temporal and spatial scales. Our dataset provides an almost unique insight into genetic change in a natural population over time and space.

Results

In order to analyze the structure of the Ammiad population over time, 100 locations were marked by pegs and by GPS coordinates, along four transects traversing seven ecologically distinct microhabitats (Anikster and Noy-Meir, 1991) (Figure 1A, Dataset S1, Movie S1). Seeds were sampled within 1 meter of each location at each of nine time points, and sown in the greenhouse for genotyping. In total, we genotyped 832 individuals using a genotyping-by-sequencing (GBS) protocol (Poland et al., 2012), resulting in 5196 single copy, single-nucleotide-polymorphism (SNP) markers that were unambiguously positioned on the wild emmer wheat reference genome (Avni et al., 2017).

We found that the population is almost entirely composed of genetically distinct groups of nearly identical, highly homozygous individuals, clustered in space. Pairwise genetic identity follows a multimodal distribution that is characterized by pairs of plants that are either effectively identical, or share at 70-90% of SNP alleles (Figure 1D). We unambiguously assigned all individuals to distinct genotype groups (DGGs) using a cut-off of >98% allele-sharing. This resulted in 118 DGGs over all nine time points, including 61 singletons (DGGs with a single member). The 10 largest DGGs encompass 65% of the samples, while the numbers of DGGs per year varied between 32 (2014) to 49 (1988; Dataset S1). Rarefaction curves indicate that the sampling scheme was sufficient to detect almost all of the DGGs present close to the transects (Figure S1). These results provide a detailed picture of the genetic structure of the population through time and space.

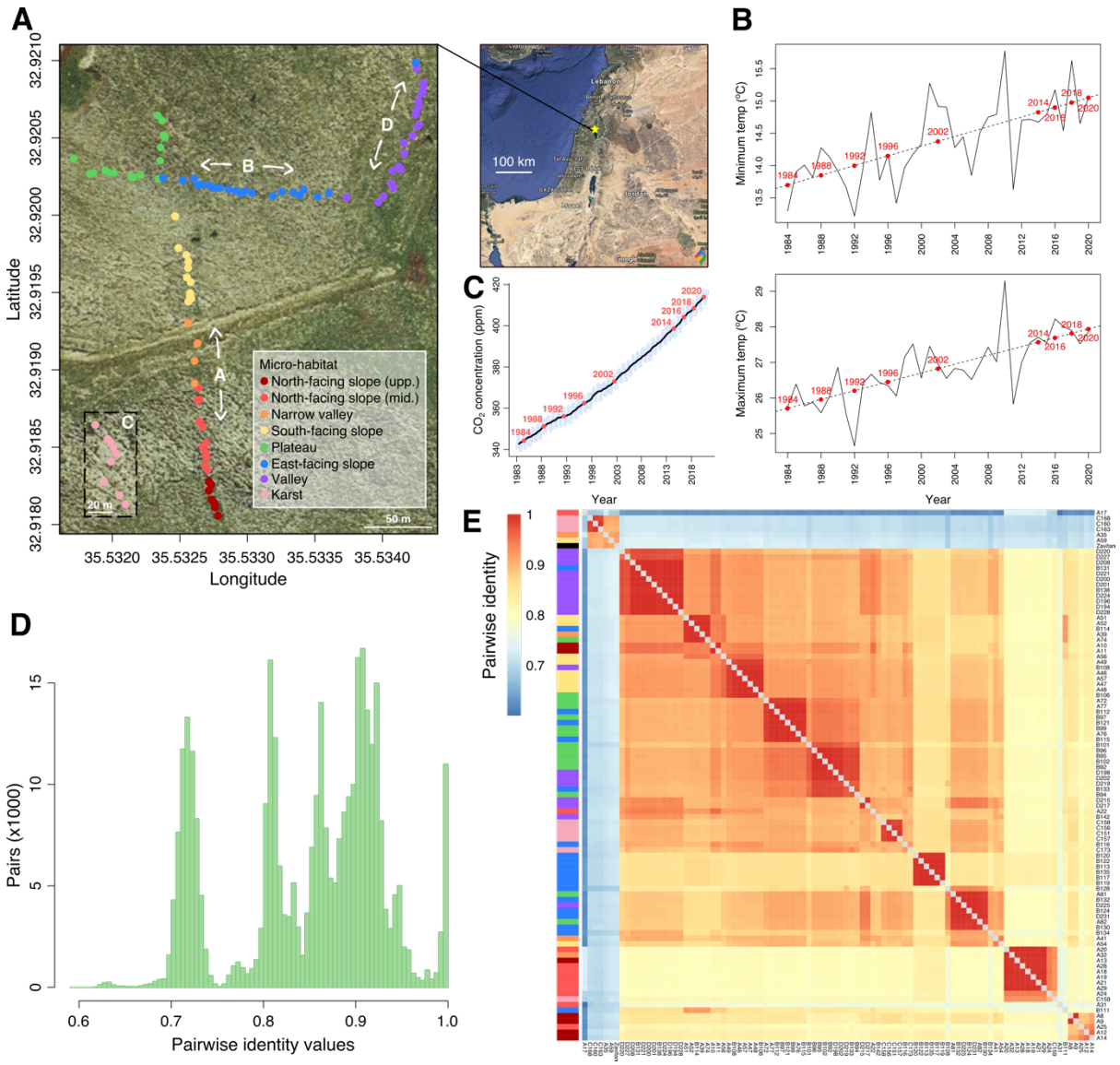

Figure 1. Ammiad population study design and spatial structure. (A) Location of Ammiad near the lake of Galilee (star, top left and geographic coordinates, bottom right). Sampling points of transects A, B, C, D collected in the years 1984, 1988, 1992, 1996, 2002, 2014, 2016, 2018 and 2020. Sampling points are shown on-site for transects A, B, D, but transect C, shown in the dashed rectangle, is located ~500 meters north-west of A, B, D. Sampling points colors correspond to the different microhabitats labeled in the legend. The map on the right is from gov.map.co.il, and the map on the left from Google Maps. (B) Average yearly minimum (top) and maximum (bottom) temperature measured in Ayelet Haschahar weather station from 1984 to 2020. Collection years are marked in red on the linear model regression line. (C) CO_2 concentration 1983 to 2021. Data obtained from the Mauna Loa record, Scripps Institution of Oceanography, UC San Diego. (D) Distribution of pairwise identity values

between the plants in the collection. (E) Population structure of Ammiad in the first year of collection (1984). Heatmap colors represent identity value for each pairwise comparison, annotation colors (on the left) correspond to the list of microhabitats in Figure 1A.

Though outcrossing is thought to be relatively low in wheat (0.5%, Golenberg, 1988) we also identified 15 (1.8%) highly heterozygous plants in Ammiad collection. Using SNPMatch (Pisupati et al., 2017), we were able to identify their parental DGGs (Figure S2B), which suggests that outcrossing happen between plants that are nearby. Based on F_{IS}, we estimated an average outcrossing rate of 3.7% across the years in Ammiad, with detectable variation between the different habitats (1.8-8.8%, Table S1). Such ranges are compatible with the estimated values (2-9%) in the literature of bread wheat (*Triticum aestivum*) using the same approach (Enjalbert and David, 2000). Interestingly, we also observed a significant two-fold decrease (p-value 0.016) in the outcrossing rates over time, from about 4.5% in 1984 to about 2% after 2016 (Figure S2A).

Returning to the inbred individuals, the spatio-temporal distribution of DGGs shows that plants of the same DGG tend to cluster together in both space and time (Figures 1E and 2). This clustering was also found in a principal component analysis (Figures 3A and 3B). Although there is little evidence for isolation by distance over the years of collection and along the transects (Figure 3C and Figure S3), within years, the probability of belonging to the same DGG decays rapidly with distance (Figure 4A). Overall, we find a striking concordance between DGGs and microhabitats, which were defined based on topographic and floristic data without knowledge of the genetic

153 structure of the population (Noy-Meir et al., 1991b) (Figure 2). For example, in transect
154 A there is a sharp transition between DGGs of the upper and middle north-facing slope
155 (Figure 2A). Another example is the genotype at collection point A59 in a unique
156 location under the shade of a *Ziziphus spina-christi* tree (Figure 2A). In contrast, in
157 transect D, where there is negligible microhabitat differentiation, plants of different
158 DGGs were much more mixed (Figure 2D). The spatial pattern was highly stable over
159 the course of the experiment. In contrast to the rapid spatial decay, the probability of
160 belonging to the same DGG decays only slowly over time (Figure 4B). For example,
161 33% of plants sampled in 1984 belonged to the same DGG as plants sampled at the
162 same position in 2020. In conclusion, our results show a strong spatial structure,
163 associated with microhabitat, which has remained stable for at least 36 years despite
164 changes in climatic conditions.

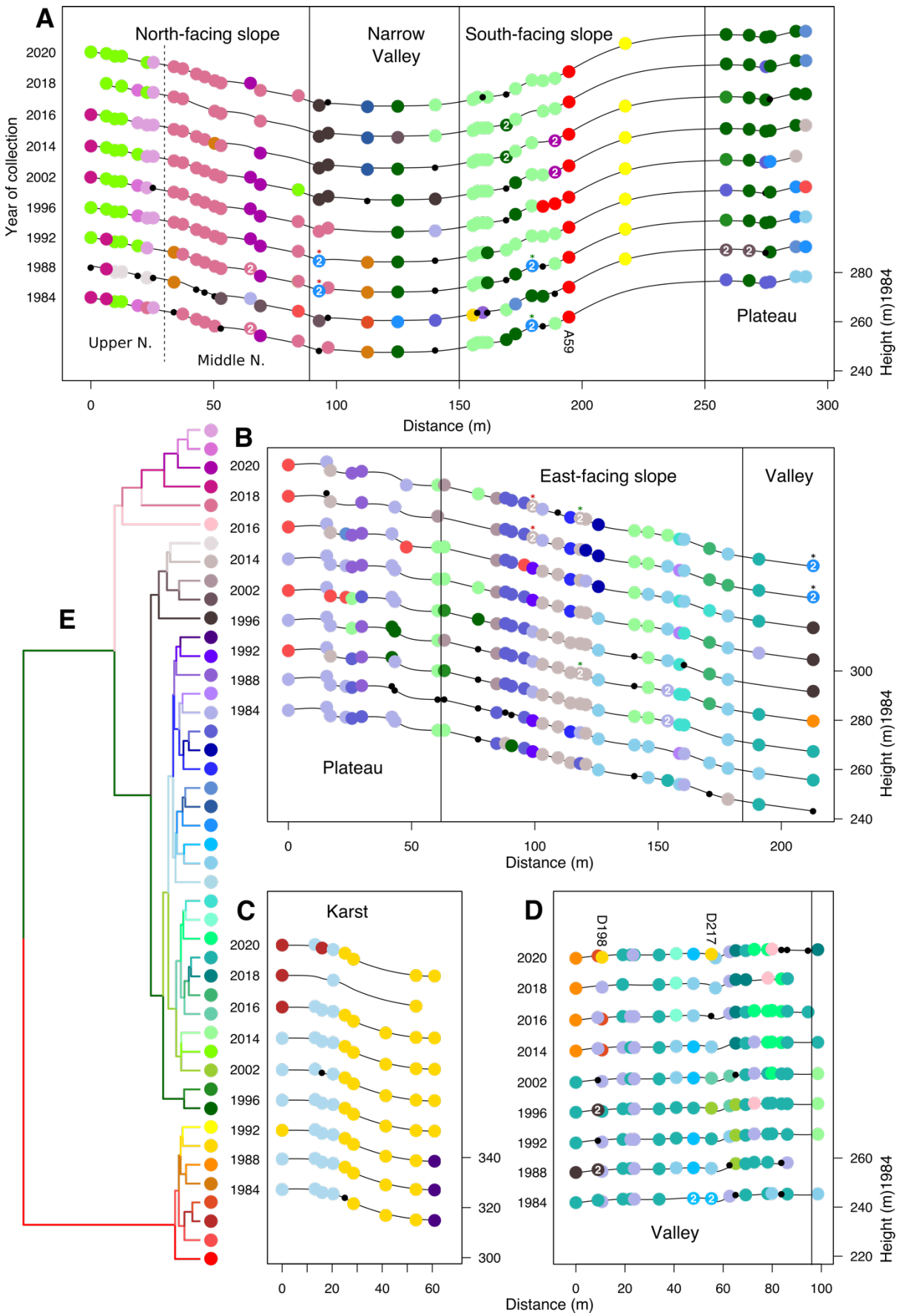
A
North-facing slope
Narrow Valley
South-facing slope
Year of collection
Upper N.
Middle N.
A59
Plateau
Height (m)1984
Distance (m)
B
East-facing slope
Valley
Plateau
C
Karst
D
D198
D217
Valley
E

165

166 **Figure 2. Spatio-temporal distribution of genotypes.** (A-D) Distribution of samples colored
167 by distinct genotype group (DGG) in transects A, B, C and D. Y-axes indicate year of collection
168 (left) and altitude for 1984 (right). Singleton samples are marked in small black dots, while
169 doubleton groups are marked with "2" in the middle with the color of their closest DGG.
170 Doubleton groups that are closest to the same DGG were marked with colored asterisks. (E)
171 Dendrogram of DGGs with ≥ 3 samples, hierarchically clustered by UPGMA.
172

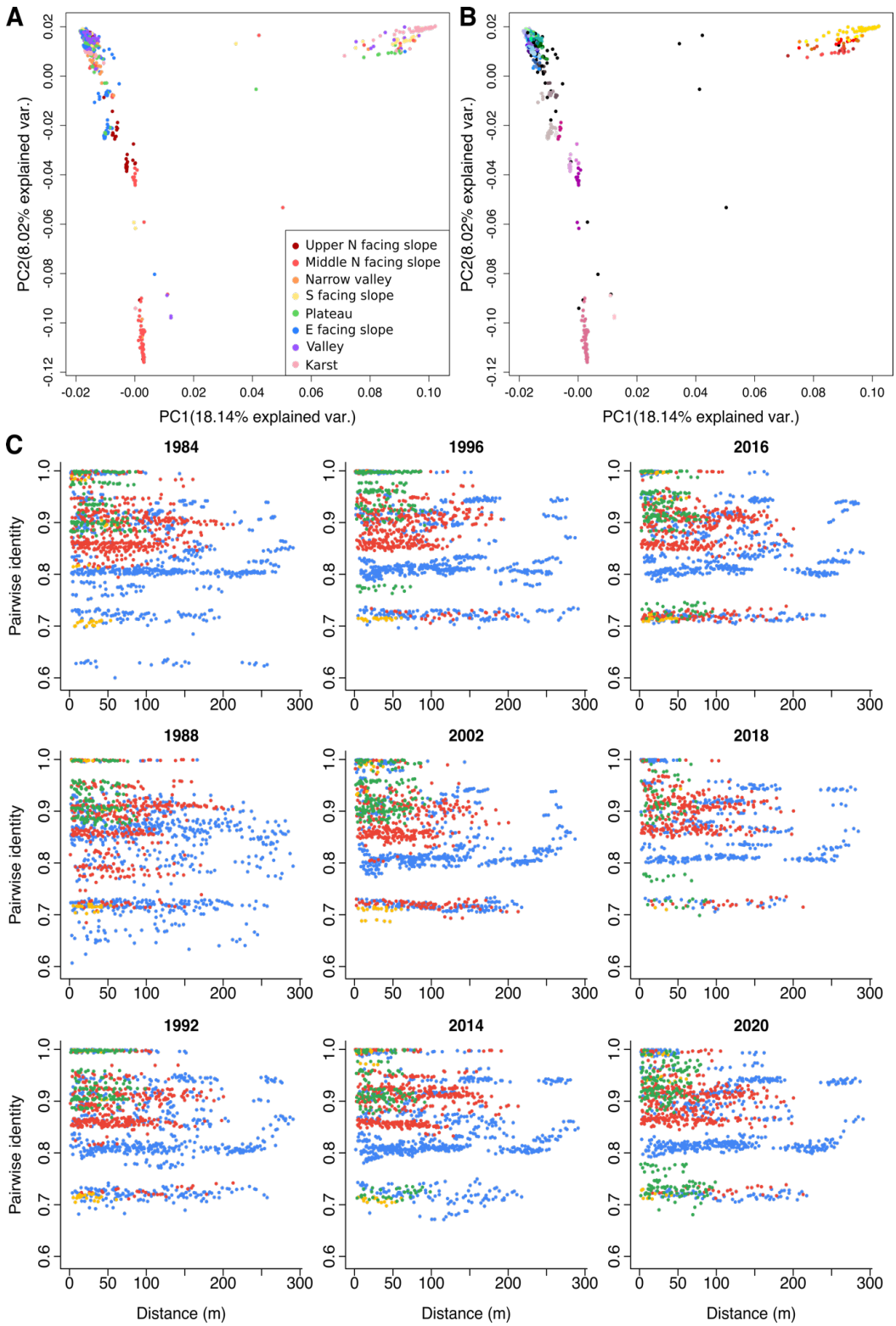

Figure 3. Principal Component Analysis (PCA) and isolation by distance of Ammiad collection. (A) PCA colored by microhabitat. (B) PCA colored by DGGs, black dots represent singleton DGGs. (B) Scatter plots of pairwise genetic identity and Euclidean distance (meters). Subplots show years of collection, and colors represent the different transects (A=blue, B=red, C=yellow, D=green).

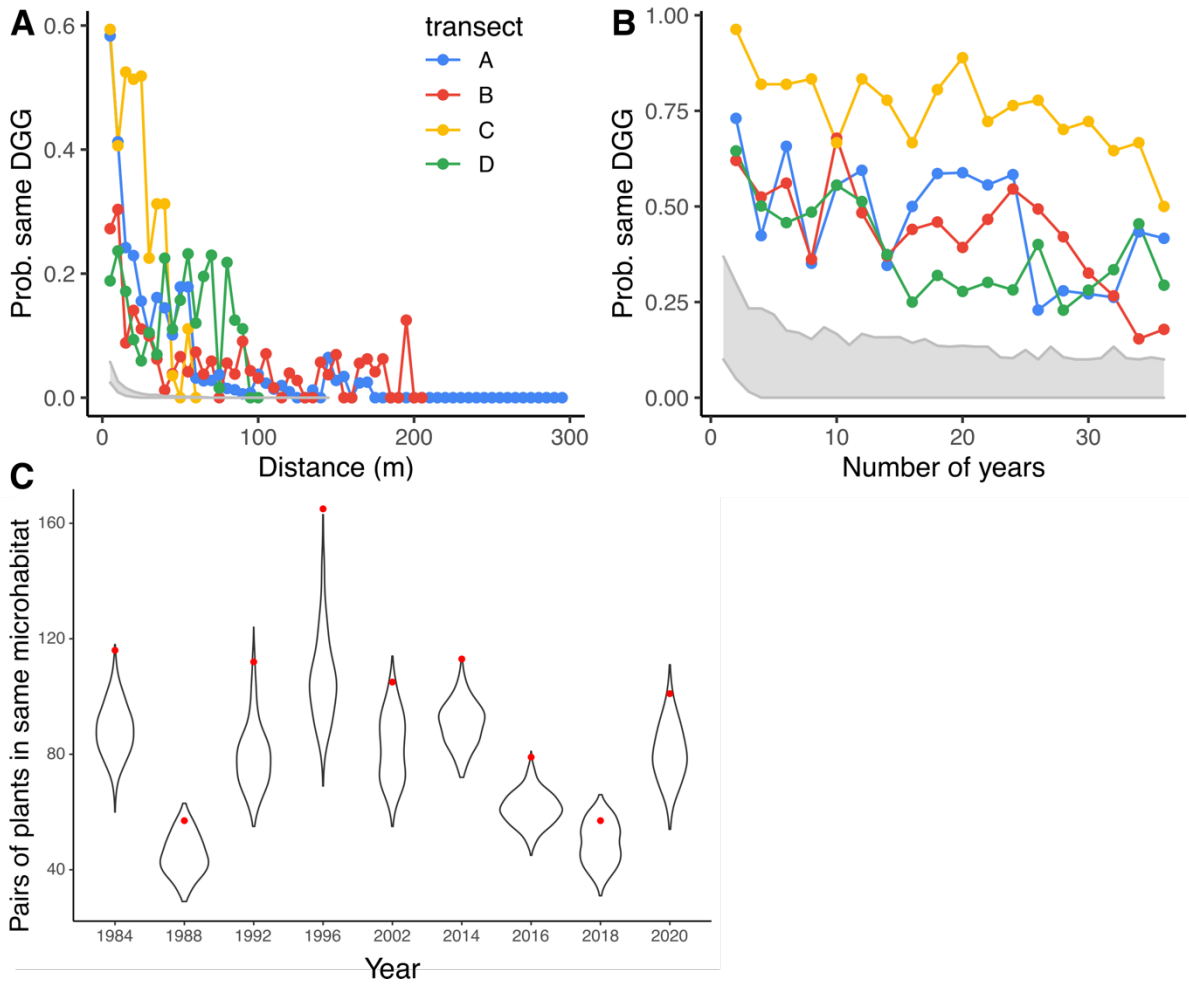

Figure 4. Spatial clustering and temporal stability at Ammiad. Points show the probability of observing genotypes of the same DGG at (A) pairs of sampling points in the same year at increasing distances along each transect and (B) the same sampling point between pairs of years. Grey regions indicate 95% confidence intervals over populations simulated under conditions closest to empirical estimates (3 plants/m^2, mean seed dispersal of 1m, 0.5% outcrossing per generation, 30% seeds germinating in the second year after dispersal). In A, points show the average for sampling points in bins of 5 meters. (C) Sorting of plants of the same DGG by microhabitat comparing observed values (red) to values obtained by permuting habitat labels (violins).

193 The observed patterns are far from random. Across transects, pairs of the same DGG
194 were significantly more likely to be found in the same microhabitat in the observed
195 dataset than in 1000 permuted datasets where the order of microhabitats was
196 randomly shuffled (Figure 4C), or even when we control for distance and spatial
197 autocorrelation using partial Mantel tests and Moran-spectral-randomization Mantel
198 statistics (MSR-Mantel) (Figures 5A and 5B). Similarly, population differentiation
199 measured by F_{st} was consistently higher between microhabitats than within, even
200 when taking distance into account (Figures 5C and 5D), and genetic distances are
201 strongly correlated with microhabitat. Furthermore, an analysis of molecular variance
202 (AMOVA) showed that 28% of the genetic variation between samples is explained by
203 differences between microhabitats (Table S2).
204 Motivated by these results, we decided to test whether it was possible to explain the
205 patterns using explicit demographic models that incorporate both self-fertilization and
206 limited dispersal. The question is whether these neutral demographic processes - on
207 their own - could generate the strong spatial clustering and temporal stability observed
208 at Ammiad.

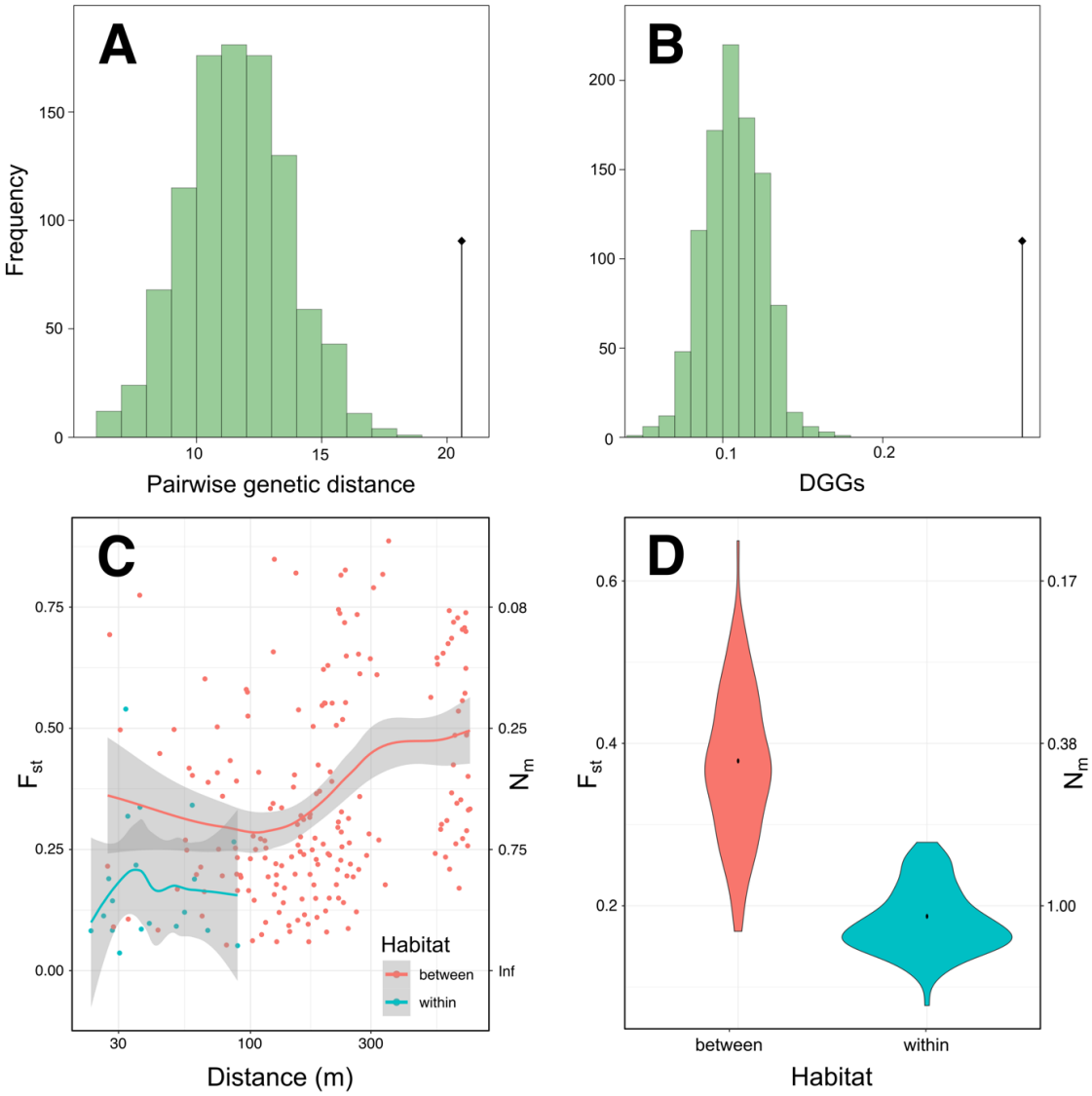

Figure 5. Genetic differentiation between and within habitats, accounting for spatial distance. (A-B) Histograms of 1000 spatially constrained randomizations of Mantel statistics (MSR-Mantel), testing for the role of habitats in determining the spatial autocorrelation in Ammiad. Observed values (black dots) versus randomizations for (A) pairwise genetic distances (p-value < 0.001) and (B) DGGs (p-value < 0.001). (C-D) Plants within each habitat were grouped in 30m demes. Pairwise F_{st} was calculated among all demes, within and between habitats. (C) Pairwise F_{st} plotted as a function of distance, measured as the average distance of plants in the two demes. Credibility intervals of a loess fit with degree 1 are shown in gray. (D) Pairwise F_{st} between demes with average distance <50m. Average observed values are shown as a black dot. Uncertainty was estimated with 1000 bootstraps of the parcels considered for the comparisons. Average within-habitat Fst was higher than between-habitat F_{st} in 3% of the bootstraps. For both C and D, Nm values (i.e. the theoretical number of migrants between parcels in an infinite island model) calculated are shown on the right axis.

223 We performed individual-based simulations of populations of plants in a homogeneous
224 environment, evolving by seed dispersal and outcrossing only. We ran simulations
225 using different values of outcrossing rate, plant density, seed dormancy and mean
226 seed dispersal distance that approximate a range of biologically realistic values.
227 Empirical values of outcrossing rates in wild wheat have been estimated to be
228 approximately 0.5% (Golenberg, 1988), and we conservatively use this value here
229 although our estimates above point to an outcrossing rate of around 3.7%, with up to
230 30% of germinating seedlings coming from the seed bank (Horovitz, 1998). Average
231 plant density in the Ammiad population was measured in 1984 as 4 plants/m^2 (Noy-
232 Meir et al., 1991a) and again in 2020 for transect A as 3.8 plants/m^2 (Dataset S1). We
233 lack direct estimates of seed dispersal, but average gene flow, a composite of seed
234 and pollen dispersal, was estimated to be 1.25 m per year (Golenberg, 1987). Seed
235 dispersal occurs through a combination of gravity, ants, birds, grazing mammals and
236 rodents, enabling both short and long-distance dispersal. For example, the
237 appearance of a DDG prominent in transect C (Figure 2C, marked by yellow dot), in
238 transect D in 2020 (Figure 2D, locations D198, D217), more than 700 meters away,
239 demonstrates that long distance movement occasionally occurs.
240 In simulations with parameters supported by observations (1 m mean seed dispersal,
241 0.5% outcrossing, density of 3 plants/m2 and 30% seed dormancy) we find that neutral
242 demographic processes alone could not account for the observed spatial clustering
243 and temporal stability (Figure 4), in line with other studies (Nevo, 2009). However, the
244 simulation could produce results consistent with the data if we assumed extremely low
245 plant densities (≤1 plant/m2) or rates of gene flow (outcrossing < 0.5% when seed
246 dispersal ≤ 1m) (Figure S4). Without better estimates of these parameters or direct

247 fitness estimates from reciprocal transplant experiments, it is not possible to definitely
248 reject a purely neutral explanation for the observed patterns. That said, the
249 correspondence between DGGs and microhabitats is strong (Figure 2, Figure 4C,
250 Figures 5C and 5D), and certainly not compatible with the outcrossing rates measured
251 in this experiment. Thus, the simulations indicate that it would be difficult to generate
252 the observed patterns of stability over 36 years through neutral demographic
253 processes alone.
254
255 In order to further examine the correspondence between DGGs and microhabitats, we
256 phenotyped 95 DGGs in a six-randomized-blocks common-garden experiment (Figure
257 6A). In order to reduce the genotype x environment effects as much as possible, plants
258 were sown in early November in their native soil brought from Ammiad site with no use
259 of fertilizers. We focused on measuring phenotypes related to yield and fecundity
260 (Figure S5).

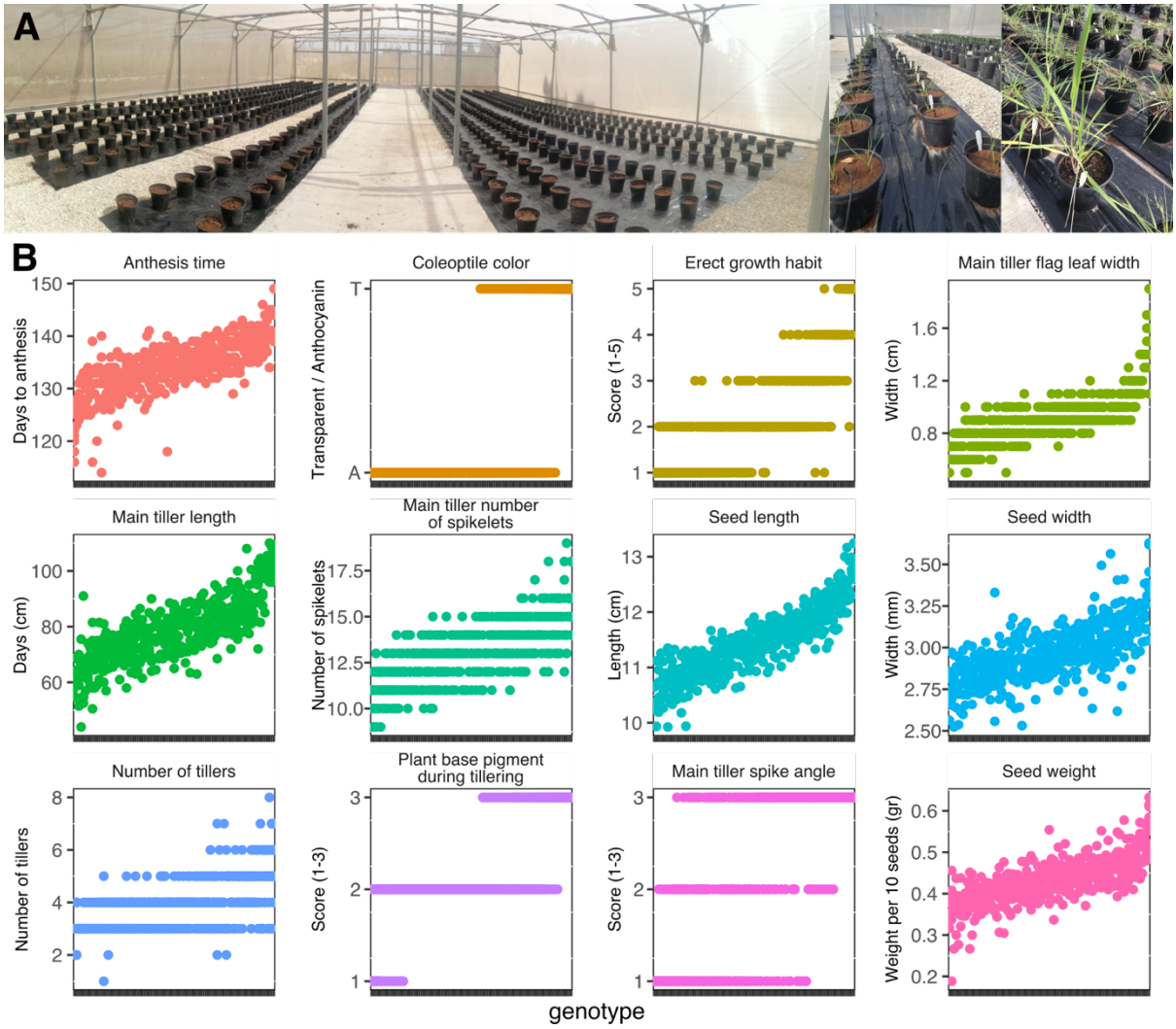

Figure 6. Phenotypes measured in the common-garden experiment. (A) Panoramic picture of the experiment site and close up pictures inside the net house in Weizmann Institute of Science. (B) Phenotypic value (y-axis) in all growing conditions (blocks) for each genotype, sorted along the mean phenotypic value of each genotype (x-axis).

We estimated the heritability of each phenotype leveraging the correlation of each genotype's phenotype across blocks, calculating the proportion of total variance explained by the genotypes vs. the residual and that explained by blocks (Figure 6B and Figure S6A). Almost all phenotypes exhibited moderate to high heritability (23-78%), with seed length the most heritable (78.0+/-3.7%). The heritability of

germination time was indistinguishable from 0, and it was therefore excluded from further analyses (after being used to calculate anthesis time, which instead showed a heritability of 50.0+/-14.5%; Table S3).

We then aimed at testing whether habitat could explain the distribution of phenotypes, while taking the distribution of genotypes into account. We assigned genotypes to different habitats, considering a genotype representative of a habitat when at least 30% of the samples were found in that specific habitat (Table S4). For each trait, we then tested whether habitat was making a significant contribution in explaining the variation between phenotypes belonging to different genotypes (see Methods). After a Bonferroni- correction for multiple testing, we observed that habitat was significantly explaining differences in coleoptile color (p-value 0.020) and plant base pigmentation during tillering (p-value 0.034). Other traits were non-significant, though a Stouffer's test, corrected for the non-independence between phenotypes (Figure S6B), supports the hypothesis that habitats explain differences between phenotypes in Ammiad (Stouffer's method with Strube's adjustment p-value=0.0118). A linear discriminant analysis confirms that coleoptile color is the most relevant trait for distinguishing between habitats, followed by main tiller length and number of tillers (Figure S7). In particular, the first dimension of the linear discriminant analysis, which explains 42.1% of the variance explained by the analysis, separates habitats with more pigmented plants and longer seeds and plants (valley and south-facing slope) from others (Figure S6C, Table S5).

297 ## Discussion

298 Studies of natural populations rarely have fine-scale geographic resolution, and almost
299 never have temporal resolution beyond the duration of a PhD (Siepielski et al., 2009).
300 Our study, spanning over 36 years of dense sampling, thus provides a unique dataset
301 that could improve our understanding of gene flow and local adaptation - often
302 modeled quite abstractly in population genetics - on an ecological scale.
303 Our analysis revealed that the Ammiad population varies more in space than in time.
304 We found unexpectedly strong long-term genetic stability, demonstrating that gene
305 flow can effectively be highly limited in a wild cereal despite its wide distribution
306 throughout the fertile crescent. Remarkably, the stable genetic clusters observed in
307 Ammiad matched ecological microhabitats previously identified at the site, suggesting
308 that natural selection, in addition to limited dispersal, contributed to shaping population
309 structure. Previous studies of wild populations have demonstrated local adaptation
310 (Abebe et al., 2015; Frachon et al., 2017; Gardiner et al., 2018; Hendrick et al., 2016;
311 Schemske, 1984; Sedlacek et al., 2016; Volis et al., 2016, 2015) over large distances,
312 but none at this spatial scale nor using long-term datasets. We also showed that the
313 differences in genotypic compositions between habitats correspond to heritable
314 differences in phenotypes, and that some of these phenotypes consistently differ
315 among habitats. This further supports the hypothesis of local adaptation at the micro-
316 environment level. Interestingly, such phenotypic differences indicate which traits are
317 important for local adaptation, and could be useful for crop improvement. Specifically,
318 we observed differences in anthocyanin content and coleoptile color, which have been
319 associated to resistance to wheat fungal diseases (Khlestkina et al., 2011), as well as
320 drought resistance (Shoeva (Tereshchenko) et al., 2012), suggesting that anthocyanin

321 biosynthesis regulation in wheat can be useful for adaptation to both biotic and abiotic
322 stress. The possibility that local adaptation occurs at such a fine spatial scale as in our
323 study is intriguing, and invites experimental confirmation on further populations.
324 In light of the apparent adaptation to microhabitats, it is notable that only minor
325 changes were seen on the temporal scale when atmospheric CO_2 increased by 70
326 ppm and temperature by 1.5^{o}C. We might have expected migration of genotypes from
327 the southern to the northern slope, for example. This genetic temporal stability could
328 be interpreted as the population not having enough time to adapt due to the rapid pace
329 of climatic changes, in which case we would expect a reduction in fitness of the
330 population. However, plant density was similar in 1984 and in 2020, suggesting that,
331 so far, this has not occurred. Alternatively, it might be that wild emmer wheat has
332 evolved to be resilient to temperature fluctuations that occurred since its speciation
333 0.8 MYA ago (Levy and Feldman, 2022) and that recent climate changes have not yet
334 reached critical levels - while local adaptation is very local indeed.
335
336 Archaeological excavations of a hunter-gatherer's site on the shore of Lake Galilee
337 uncovered an abundant wild emmer wheat, indicating that it has been present in the
338 region of Ammiad for at least 23,000 years (Snir et al., 2015). Since then, the Levant
339 has undergone major climatic changes, including several cycles of glaciation, warming
340 and cooling (Zeder, 2011), pointing to the robustness of wild emmer wheat.
341 Nevertheless, temperatures and atmospheric CO_2 concentrations have never been as
342 high as they are now during that period, therefore, it is unclear to what extent additional
343 changes in environmental conditions could occur before negative consequences for
344 population fitness became apparent.

345 Our results are relevant to conservation strategies as well as to the assessment of
346 biodiversity resilience under climate change. First, our study shows that *in-situ*
347 conservation can be quite effective in preserving diversity, without the need to
348 frequently sample seeds and store them in seed banks (*ex-situ*). Second, our results
349 highlight that effective *in-situ* and *ex-situ* conservation strategies of wild plants
350 biodiversity, particularly for wild grasses and crop progenitors such as wild emmer
351 wheat, should consider habitat diversity as a potential reservoir of adaptive diversity.
352 In fact, our long-term study would not have been possible if the site had not been
353 declared a natural reserve for wild-wheat conservation by the Israel nature and parks
354 authority. Indeed, this population is fenced and undergoes moderate grazing.
355 Unrestricted grazing, or urbanization, as seen in other parts of the Levant can reduce
356 and sometimes eliminate wild grasses. The Ammiad reserve is relatively small (~10
357 hectares), but contains much diversity. Establishing natural reserves of crop
358 progenitors, partially protected from anthropogenic activities, does not necessarily
359 require large areas and is a feasible goal that is critical for biodiversity conservation.
360
361 In conclusion, we provide a unique example of strong temporary stability in a wild
362 grass population, most likely due to a combination of local adaptation and limited
363 dispersal. This stability is remarkable given that, during the period of this study,
364 temperatures and CO_2 levels increased significantly (Figures 1B and 1C). Yet only
365 rather minor changes occurred in the population genetic structure, reflecting the ability
366 of wild plants to deal with changing environments and pointing to the robustness of
367 wild emmer wheat. Such robustness further demonstrates the importance of

368 conservation of wild relatives of crops in nature, as gene pools for breeding (Zsögön
369 et al., 2021).
370

371 ## Materials and Methods

372 ### Sample collection and DNA extraction

373 Wild wheat spikes were collected in four different linear transects every 3 to 5 meters
374 from sampling points marked with pegs and GPS coordinates (Dataset S1). Plants
375 were assigned to a sampling point when collected in successive years in a radius of ~
376 1m from the peg. A single seed was selected for each plant and DNA was extracted
377 from young seedlings. Tissue was collected and ground using mortar and pestle with
378 the addition of Merck sea sand in liquid nitrogen. DNA extraction was done using
379 Macherey-Nagel NucleoSpin® Plant II extraction kit, according to the manufacturer's
380 protocol, eluting in 50 ul EB total. Concentrations and DNA quality were estimated
381 using a NanoDrop® ND-1000 Spectrophotometer.

382 ### Genotyping by sequencing (GBS) and variant calling

383 Plant genotyping was done according to the Genotyping-By-Sequencing method
384 (Elshire et al., 2011; Poland et al., 2012). Samples were sequenced using Illumina
385 NextSeq 550 mid-output 150 base-pairs single-end kits. A reference sample, Zavitan
386 accession (Avni et al., 2017), was added to each run, undergoing the same plate GBS
387 library preparation and sequencing. Samples were divided by barcodes using a python
388 2.7 code. Mapping to the WEW_v2.0 genome assembly (Zhu et al., 2019) was done
389 using *bwa-mem* (Li, 2013). Conversion to binary alignment map (BAM) format, filtering

390 for uniquely mapped reads with minimum QUAL score of 30, sorting and indexing was
391 done using SAMtools (Li et al., 2009). Variant calling was done in parallel running on
392 all 845 (832 Ammiad samples and 13 Zavitan controls) samples using GATK
393 HaplotypeCaller 3.8 (Poplin et al., 2018). Filtering for quality (>30), read depth (>6),
394 genotype quality (>15), maximum missing sites (10%) and no-indels was done using
395 VCFtools (Danecek et al., 2011). Filtering for up to 10% heterozygous plants per
396 polymorphic position was done using TASSEL5 (Bradbury et al., 2007). Filtered VCF
397 was used for all further analyses.

398 **Pairwise genetic identity**

399 Identity was measured using R code which calculates the pairwise identity values
400 between all samples, divided by the numbers of comparisons. The pipeline also
401 includes the division of the samples to distinct genotype groups (DGGs), done by
402 setting a threshold of 98.1% identity, which is the lowest threshold where no sample
403 is assigned to two or more DGGs, and the construction of the dendrogram describing
404 the relatedness between the DGGs. Hierarchical clustering was done in R by UPGMA.
405 The 13 Zavitan reference samples added to each run were grouped together with
406 99.4% identity. Heatmap of samples from 1984 was done using *pheatmap*
407 (https://cran.r-project.org/web/packages/pheatmap/index.html) with default
408 hierarchical clustering.

409 **Temperature and CO_2 concentration data**

410 Data of daily minimum and maximum temperature from 1984 to 2020 were obtained
411 from Israel Meteorological Service at the Israel government portal
412 (https://ims.data.gov.il/he/ims/2). Data of weekly atmospheric CO2 concentrations

413 were obtained from The Scripps Institution of Oceanography UC San Diego (Keeling
414 et al., 2001).

415 **Rarefaction, principal component and identity by distance analyses**

416 Rarefaction analysis was done using R, sampling backwards by the number of
417 samples and different genotypes, per year, 100 times and adjusting a polynomial to
418 each sampling.
419 Principal component analysis was done on the .vcf file of the entire Ammiad collection
420 using *SNPRelate* R Package (Zheng et al., 2012). Identity by distance was correlated
421 for each transect separately. Pairwise Euclidean distances was calculated using the
422 *distHaversine* function of *Geosphere* R package
423 (https://cran.rproject.org/web/packages/geosphere/index.html). Mantel test with 1000
424 permutations was used to calculate correlation between the genetic identity and the
425 Euclidean distance matrices, using *mantel.test* in *Ape* R package (Paradis et al.,
426 2004).
427

428 **Outcrossing estimation and parental lines detection**

429 To estimate outcrossing, we calculated F_{IS} using the R package hierfstat. Confidence
430 intervals were calculated using 100 bootstraps and quantiles 2.5% and 97.5% using
431 the function boot.ppfis. F_{IS} estimates were used to estimate outcrossing rates *f* using
432 the relationship $F_{IS} = (1-f)/(1+f)$ (Wright, 1969). In order to detect the parental DGGs
433 of heterozygous plants, we have used SNPMatch (Pisupati et al., 2017), running one
434 plant against all DGGs.

435 **Individual-based simulations**

436 To investigate whether neutral demographic processes could account for the observed
437 spatial clustering and temporal stability we performed individual-based simulations of
438 populations of plants evolving via seed dispersal and outcrossing only. Briefly, we
439 allow populations to evolve in a 2-dimensional continuous space, then draw a transect
440 through the population and sample plants close to 30 evenly spaced sampling points
441 in the last 36 generations to replicate the sampling procedure in the empirical dataset.
442 An R package, *simmiad*, is provided to perform these simulations
443 (DOI:10.5281/zenodo.4762083).

444 Populations begin with N plants of a single genotype distributed randomly through a
445 homogeneous habitat with 1, 2, 3 or 5 plants/m^2. At each generation, N plants are
446 sampled with replication to produce N seeds. Wild emmer wheat has a two-year seed
447 bank, so from generation 3 onwards, seeds are drawn from the previous generation
448 with probability *p*, and from two generations previous with probability 1-*p,* for values of
449 *p* of 0.5, 0.7, 0.9 or 1 .Since we are only concerned with tracking unique genotypes,
450 and information about seed dispersal is in any case lacking model outcrossing as
451 analogous to mutation; seeds are randomly assigned as outcrossed with probabilities
452 0.25%, 0.5%, 1%, or 2%, in which case it is assigned a new unique genotype.
453 Offspring disperse from the mother in a random direction at a distance drawn from an
454 exponential distribution with a mean of 0.5, 0.75, 1 or 2m. To eliminate edge effects,
455 the habitat is modelled as a torus, such that if dispersal takes a seed over the edge of
456 the habitat it is reflected back to the opposite side. We allowed populations to evolve
457 for 2000 generations to ensure populations had reached equilibrium. We then drew a
458 transect of 30 sampling points 5m apart through the middle of the population, and

459 sampled the plant closest to each sampling point in each of the final 36 generations of
460 the simulations, replicating the sampling procedure in the field. For each combination
461 of plant densities, outcrossing rates, seed bank parameter *p*, and seed dispersal
462 distances we performed 100 replicate simulations.

463 **Microhabitat sorting and analysis**

464 We aimed to test the hypothesis that the population structure of Ammiad wild wheat
465 reflects that of microhabitats. We tested this using two different statistics and
466 permutation schemes. First, we tested whether plants in the same DGG tend to be
467 confined to a single microhabitat more than would be expected by chance using a
468 procedure analogous to a permutation test. We concatenated microhabitat and DGG
469 labels across transects, and calculated how often pairs of plants of the same DGG
470 were located in the same microhabitat. We then shuffled the order of microhabitats,
471 whilst keeping labels of the same microhabitat together, and recalculated how many
472 pairs of plants of the same DGG were located in the same microhabitat after shuffling.
473 We repeated this shuffling procedure 1000 times, and compared the observed number
474 of matching pairs within the same microhabitat to the distribution of shuffled datasets.
475 This procedure randomizes the relationship between the locations of DGGs and
476 microhabitat boundaries, but maintains the overall spatial structure of DGGs and
477 microhabitats.
478 Second, we tested whether population differentiation, measured by F_{st}, is higher when
479 measured between plants occurring in different microhabitats than in the same
480 microhabitat. To this goal we subdivided plants into demes with a maximum distance
481 between plants of 30m. We then computed the pairwise Fst between demes using the

482 R package *pegas* (Paradis, 2010). To correct for the effects of isolation by distance
483 and spatial structure we stratified comparisons by distance, measured as the distance
484 between the average locations of plants in the two demes.
485 We computed an analysis of molecular variance using the R package *pegas* (Paradis,
486 2010), using plants sampled across all years and restricting the analysis only to
487 genotypes present in Ammiad. We included two factors, microhabitat and year of
488 collection, with the latter nested within the former.
489 To account for spatial autocorrelation we first performed a partial Mantel test using the
490 function *multi.mantel* from the R package *phytools* (Revell, 2012). Specifically, we
491 considered as a response variable the pairwise genetic distances used to define
492 DGGs. We tested for the effect of habitat, represented as a distance matrix with value
493 "0" for plants found in the same microhabitat and "1" for plants found in two different
494 microhabitats. In addition, we included in the test a matrix of time distances between
495 the sampling of two plants (distance measured in years) and spatial distance,
496 measured in meters and obtained from latitude and longitude using the function
497 *earth.dist* from the R package *fossil* (https://palaeo-
498 electronica.org/2011_1/238/index.html). We detected a significant effect of space and
499 microhabitat (p-values <0.005 for both matrices) and a non-significant effect of time
500 (p-value 0.863).
501 Note that Mantel and partial Mantel tests have severely been criticized for their
502 inaccuracy in presence of high spatial autocorrelation (Crabot et al., 2019; Legendre
503 et al., 2015). To account for these known biases, we used the approach proposed by
504 (Crabot et al., 2019), which leverages a Moran spectral randomization procedure to
505 generate random samples which maintain the same autocorrelation properties of the

original dataset. To this goal, we used the R packages *sdpep* to process the spatial matrices and the *msr* function of the package *adespatial* (Guénard and Legendre, 2022). The distances above were transformed into Euclidean distances with function *cailliez* from the R package *adegenet* (Jombart and Ahmed, 2011). Using this approach, we tested the effect of habitat on both DGGs and pairwise genetic distances, using 1000 randomizations. In both cases the effect of microhabitat was significant (p-value<0.05).

Common garden experiment and analysis

We established a six-randomized-blocks common garden experiment in a net-house in the Weizmann Institute of Science. In order to keep conditions as similar as possible to the conditions in Ammiad site, seeds were sown in mid-November, in Terra Rosa soil that was brought from Ammiad location and the experiment was subjected to winter rainfall. We chose 95 samples representing 95 DGGs, not including DDGs of heterozygous singletons. Phenotypes measured were: germination date, coleoptile color (anthocyanin pigment/no pigment), erect growth habit (scored from 1 to 5), plant base pigment during tillering (scored from 1 to 3), anthesis date, phenotypes during anthesis - main tiller length (cm) from the soil to the basis of the spike, main tiller flag leaf width (cm), main tiller number of spikelets, main tiller spike angle (scored from 1 to 3) and number of tillers. After seed collection we measured dry seed phenotypes of 10 seeds per plant: seed area (mm^2), seed length (mm), seed width (mm) and 10 seeds' weight (gr).

Phenotypic analyses were done in R (https://github.com/TalDM/Ammiad/tree/main/data_analysis/phenotypes.R).

530 Heritability estimates were performed using the R package *brms* (Bürkner, 2017),
531 implementing a linear mixed model with both genotypes and block as random factors.
532 For coleoptile color we implemented a logistic linear mixed model. Heritability was
533 calculated as var_g/(var_g+var_b+var_r), where var_g indicates the variance
534 explained by genotypes, var_b that explained by blocks, and var_r the residual
535 variance. Tests of the role of habitat were performed using the R package *lme4* (Bates
536 et al., 2015), testing an analogous model to that used to calculate heritability versus a
537 model including habitat as an additional fixed factor, using the R function anova.
538 Specifically, we tested models with the structure
539 "phenotype~habitats+(1|block)+(1|new_dgg)" vs. a set of null models not including the
540 factor habitats.
541 Stouffer's test was calculated using the R package *poolr* (Cinar and Viechtbauer,
542 2022). The linear discriminant analysis was computed and evaluated using the R
543 package *caret* (Kuhn, 2008). Linear discriminant analyses were computed using the
544 R function caret, after z-transformation of all the phenotypic data.

545 Data and code availability

546 Sequencing data generated in this study are available in the National Center for
547 Biotechnology Information (NCBI) Sequence Read Archive (SRA) under the accession
548 number PRJNA779576. All data processing and data analysis are publicly available
549 on GitHub (https://github.com/TalDM/Ammiad). An R package, *simmiad*, is provided
550 to perform the individual-based simulations (DOI:10.5281/zenodo.4762083).
551
552

553 ## Author Contributions

554 T.D-M., M.F., Y.A. and A.A.L, conceived and designed the study. T.D-M. carried out
555 the molecular work, SNP calling, genetic and phenotypic analyses with input from
556 T.J.E., F.M., M.N. and A.A.L. T.J.E. performed the simulations and microhabitat
557 sorting analyses with input from T.D-M., M.N. and A.A.L. F.M. carried out the
558 population differentiation analysis, the MSR-Mantel tests and the phenotypic analyses
559 with input from T.D-M. and A.A.L. T.D-M., O.R. and A.A.L, carried out the common-
560 garden experiment. T.D-M., H.S., J.M., N.A-R., A.R., M.F., Y.A, and A.A.L carried out
561 the collection. T.D-M., T.J.E., F.M, M.N. and A.A.L wrote the manuscript. M.N. and
562 A.A.L supervised the project.

563

564 ## Competing Interest Statement

565 The authors declare no competing interests.

566 ## Acknowledgements

567 We thank T. Azulay, T. Grinevich, C. Melamed-Bessudo, O. Gross, R. Epstein, Z. Meir
568 and members from the Institute for Cereal Crops Improvement at Tel-Aviv University
569 for plant material collection and J. Müller for the drone movie. We also thank D. Filiault,
570 K. Swarts, S. Nowoshilow, N. De-Malach, R. Pisupati, R. Burns, Y. Voichek, P. Clauw,
571 E. Kosman and the Levy and Nordborg labs for fruitful discussions.

Funding

This work was supported by the Yeda-Sela Center and Sustainability and Alternative Energy Research Initiative of the Weizmann Institute of Science. T.D-M. acknowledges a European Molecular Biology Organization scientific exchange grant 8368.

References

Abebe TD, Naz AA, Léon J. 2015. Landscape genomics reveal signatures of local adaptation in barley (Hordeum vulgare L.). *Front Plant Sci* **6**:813.

Aguillon SM, Fitzpatrick JW, Bowman R, Schoech SJ, Clark AG, Coop G, Chen N. 2017. Deconstructing isolation-by-distance: The genomic consequences of limited dispersal. *PLOS Genet* **13**:e1006911.

Anikster Y, Noy-Meir I. 1991. The wild-wheat field laboratory at Ammiad. *Isr J Bot* **40**:351–362.

Ashraf B, Hunter DC, Bérénos C, Ellis PA, Johnston SE, Pilkington JG, Pemberton JM, Slate J. 2021. Genomic prediction in the wild: A case study in Soay sheep. *Mol Ecol*.

Avni R, Nave M, Barad O, Baruch K, Twardziok SO, Gundlach H, Hale I, Mascher M, Spannagl M, Wiebe K, Jordan KW, Golan G, Deek J, Ben-Zvi B, Ben-Zvi G, Himmelbach A, MacLachlan RP, Sharpe AG, Fritz A, Ben-David R, Budak H, Fahima T, Korol A, Faris JD, Hernandez A, Mikel MA, Levy AA, Steffenson B, Maccaferri M, Tuberosa R, Cattivelli L, Faccioli P, Ceriotti A, Kashkush K, Pourkheirandish M, Komatsuda T, Eilam T, Sela H, Sharon A, Ohad N, Chamovitz DA, Mayer KFX, Stein N, Ronen G, Peleg Z, Pozniak CJ, Akhunov ED, Distelfeld A. 2017. Wild emmer genome architecture and diversity elucidate wheat evolution and domestication. *Science* **357**:93–97.

Bates D, Mächler M, Bolker BM, Walker SC. 2015. Fitting Linear Mixed-Effects Models Using lme4. *J Stat Softw* **67**:1–48. doi:10.18637/JSS.V067.I01

Bradbury PJ, Zhang Z, Kroon DE, Casstevens TM, Ramdoss Y, Buckler ES. 2007. TASSEL: software for association mapping of complex traits in diverse samples. *Bioinformatics* **23**:2633–2635.

Bürkner PC. 2017. brms: An R Package for Bayesian Multilevel Models Using Stan.

604 *J Stat Softw* **80**:1–28.

605 **Chen N, Juric I, Cosgrove EJ, Bowman R, Fitzpatrick JW, Schoech SJ, Clark**
606 **AG, Coop G.** 2019. Allele frequency dynamics in a pedigreed natural
607 population. *Proc Natl Acad Sci U S A* **116**:2158–2164.

608 **Cinar O, Viechtbauer W.** 2022. The poolr Package for Combining Independent and
609 Dependent p Values. *J Stat Softw* **101**:1–42.

610 **Crabot J, Clappe S, Dray S, Datry T.** 2019. Testing the Mantel statistic with a
611 spatially-constrained permutation procedure. *Methods Ecol Evol* **10**:532–540.

612 **Danecek P, Auton A, Abecasis G, Albers CA, Banks E, DePristo MA, Handsaker**
613 **RE, Lunter G, Marth GT, Sherry ST, McVean G, Durbin R, Group 1000**
614 **Genomes Project Analysis.** 2011. The variant call format and VCFtools.
615 *Bioinformatics* **27**:2156–2158.

616 **Elshire RJ, Glaubitz JC, Sun Q, Poland JA, Kawamoto K, Buckler ES, Mitchell**
617 **SE.** 2011. A Robust, Simple Genotyping-by-Sequencing (GBS) Approach for
618 High Diversity Species. *PLoS One* **6**:e19379.

619 **Enjalbert J, David JL.** 2000. Inferring recent outcrossing rates using multilocus
620 individual heterozygosity: application to evolving wheat populations. *Genetics*
621 **156**:1973–1982.

622 **Felsenburg T, Levy AA, Galili G, Feldman M.** 1991. Polymorphism of high-
623 molecular-weight glutenins in wild tetraploid wheat: spatial and temporal
624 variation in a native site. *Isr J Bot* **40**:451–479.

625 **Frachon L, Libourel C, Villoutreix R, Carrère S, Glorieux C, Huard-Chauveau C,**
626 **Navascués M, Gay L, Vitalis R, Baron E, Amsellem L, Bouchez O, Vidal M,**
627 **Le Corre V, Roby D, Bergelson J, Roux F.** 2017. Intermediate degrees of
628 synergistic pleiotropy drive adaptive evolution in ecological time. *Nat Ecol Evol*
629 *2017 110* **1**:1551–1561.

630 **Franks SJ, Sim S, Weis AE.** 2007. Rapid evolution of flowering time by an annual
631 plant in response to a climate fluctuation. *Proc Natl Acad Sci* **104**:1278–1282.

632 **Fu Y-B, Peterson GW, Horbach C, Konkin DJ, Beiles A, Nevo E.** 2019. Elevated
633 mutation and selection in wild emmer wheat in response to 28 years of global
634 warming. *Proc Natl Acad Sci* **116**:20002–20008.

635 **Gardiner LJ, Joynson R, Omony J, Rusholme-Pilcher R, Olohan L, Lang D, Bai**
636 **C, Hawkesford M, Salt D, Spannagl M, Mayer KFX, Kenny J, Bevan M, Hall**
637 **N, Hall A.** 2018. Hidden variation in polyploid wheat drives local adaptation.
638 *Genome Res* **28**:1319–1332.

Golenberg EM. 1988. Outcrossing rates and their relationship to phenology in Triticum dicoccoides. *Theor Appl Genet* **75**:937–944.

Golenberg EM. 1987. Estimation of gene flow and genetic neighborhood size by indirect methods in a selfing annual, Triticum dicoccoides. *Evolution (N Y)* **41**:1326–1334.

Guénard G, Legendre P. 2022. Hierarchical Clustering with Contiguity Constraint in R. *J Stat Softw* **103**:1–26.

Hendrick MF, Finseth FR, Mathiasson ME, Palmer KA, Broder EM, Breigenzer P, Fishman L. 2016. The genetics of extreme microgeographic adaptation: an integrated approach identifies a major gene underlying leaf trichome divergence in Yellowstone Mimulus guttatus. *Mol Ecol* **25**:5647–5662.

Hoffmann AA, Sgró CM. 2011. Climate change and evolutionary adaptation. *Nat 2011 4707335* **470**:479–485.

Horovitz A. 1998. The soil seed bank in wild emmerThe Proceedings of International Symposium of In Situ Conservation of Plant Genetic Diversity. pp. 185–188.

Horovitz A, Feldman M. 1991. Evaluation of the wild-wheat study at Ammiad. *Isr J Bot* **40**:501–508.

Jombart T, Ahmed I. 2011. adegenet 1.3-1: new tools for the analysis of genome-wide SNP data. *Bioinformatics* **27**:3070–3071.

Keeling CD, Piper SC, Bacastow RB, Wahlen M, Whorf TP, Heimann M, Meijer HA. 2001. Exchanges of Atmospheric CO2 and 13CO2 with the Terrestrial Biosphere and Oceans from 1978 to 2000. I. Global Aspects. *I Glob Asp SIO Ref Ser* **Scripps In**:88.

Khlestkina E, Antonova E, Pershina L, Soloviev A, Badaeva E, Börner A, Salina E. 2011. Variability of Rc (red coleoptile) Alleles in Wheat and Wheat-alien Genetic Stock Collections. *Cereal Res Commun 2011 394* **39**:465–474.

Khoury CK, Carver D, Greene SL, Williams KA, Achicanoy HA, Schori M, León B, Wiersema JH, Frances A. 2021. Crop wild relatives of the United States require urgent conservation action. *Proc Natl Acad Sci U S A* **117**:33351–33357.

Kolis KM, Berg CS, Nelson TC, Fishman L. 2022. Population genomic consequences of life-history and mating system adaptation to a geothermal soil mosaic in yellow monkeyflowers. *Evolution (N Y)* **76**:765–781.

Kuhn M. 2008. Building Predictive Models in R Using the caret Package. *J Stat Softw* **28**:1–26.

674 **Legendre P, Fortin MJ, Borcard D.** 2015. Should the Mantel test be used in spatial
675 analysis? *Methods Ecol Evol* **6**:1239–1247. doi:10.1111/2041-210X.12425

676 **Levy AA, Feldman M.** 2022. Evolution and origin of bread wheat. *Plant Cell*.

677 **Levy AA, Feldman M.** 1988. Ecogeographical distribution of HMW glutenin alleles in
678 populations of the wild tetraploid wheat Triticum turgidum var. dicoccoides.
679 *Theor Appl Genet* **75**:651–658.

680 **Li H.** 2013. Aligning sequence reads, clone sequences and assembly contigs with
681 BWA-MEM.

682 **Li H, Handsaker B, Wysoker A, Fennell T, Ruan J, Homer N, Marth G, Abecasis**
683 **G, Durbin R, Subgroup 1000 Genome Project Data Processing.** 2009. The
684 Sequence Alignment/Map format and SAMtools. *Bioinformatics* **25**:2078–2079.

685 **Nevo E.** 2009. Evolution in action across life at “Evolution Canyons”, Israel. *Trends*
686 *Evol Biol* **1**:e3–e3.

687 **Noy-Meir I, Agami M, Anikster Y.** 1991a. Changes in the population density of wild
688 emmer wheat (Triticum turgidum var. dicoccoides) in a mediterranean
689 grassland. *Isr J Bot* **40**:385–395.

690 **Noy-Meir I, Agami M, Cohen E, Anikster Y.** 1991b. Floristic and ecological
691 differentiation of habitats within a wild wheat population at Ammiad. *Isr J Bot*
692 **40**:363–384.

693 **Ozbek O, Millet E, Anikster Y, Arslan O, Feldman M.** 2007. Spatio-temporal
694 genetic variation in populations of wild emmer wheat, Triticum turgidum ssp.
695 dicoccoides, as revealed by AFLP analysis. *Theor Appl Genet 2007 1151*
696 **115**:19–26.

697 **Paradis E.** 2010. pegas: an R package for population genetics with an integrated-
698 modular approach. *Bioinformatics* **26**:419–420.

699 **Paradis E, Claude J, Strimmer K.** 2004. APE: Analyses of phylogenetics and
700 evolution in R language. *Bioinformatics* **20**:289–290.

701 **Pecl GT, Araújo MB, Bell JD, Blanchard J, Bonebrake TC, Chen IC, Clark TD,**
702 **Colwell RK, Danielsen F, Evengård B, Falconi L, Ferrier S, Frusher S,**
703 **Garcia RA, Griffis RB, Hobday AJ, Janion-Scheepers C, Jarzyna MA,**
704 **Jennings S, Lenoir J, Linnetved HI, Martin VY, McCormack PC, McDonald**
705 **J, Mitchell NJ, Mustonen T, Pandolfi JM, Pettorelli N, Popova E, Robinson**
706 **SA, Scheffers BR, Shaw JD, Sorte CJB, Strugnell JM, Sunday JM, Tuanmu**
707 **MN, Vergés A, Villanueva C, Wernberg T, Wapstra E, Williams SE.** 2017.
708 Biodiversity redistribution under climate change: Impacts on ecosystems and
709 human well-being. *Science* **355**.

Pisupati R, Reichardt I, Seren Ü, Korte P, Nizhynska V, Kerdaffrec E, Uzunova K, Rabanal FA, Filiault DL, Nordborg M. 2017. Verification of Arabidopsis stock collections using SNPmatch, a tool for genotyping high-plexed samples. *Sci Data* **4**:170184.

Poland JA, Brown PJ, Sorrells ME, Jannink J-L. 2012. Development of High-Density Genetic Maps for Barley and Wheat Using a Novel Two-Enzyme Genotyping-by-Sequencing Approach. *PLoS One* **7**:e32253.

Poplin R, Ruano-Rubio V, DePristo MA, Fennell TJ, Carneiro MO, Auwera GA Van der, Kling DE, Gauthier LD, Levy-Moonshine A, Roazen D, Shakir K, Thibault J, Chandran S, Whelan C, Lek M, Gabriel S, Daly MJ, Neale B, MacArthur DG, Banks E. 2018. Scaling accurate genetic variant discovery to tens of thousands of samples. *bioRxiv* 201178.

Revell LJ. 2012. phytools: an R package for phylogenetic comparative biology (and other things). *Methods Ecol Evol* **3**:217–223.

Schemske DW. 1984. Population structure and local selection in Impatiens pallida (balsaminaceae), a selfing annual. *Evolution (N Y)* **38**:817–832.

Sedlacek J, Cortés AJ, Wheeler J, Bossdorf O, Hoch G, Klápště J, Lexer C, Rixen C, Wipf S, Karrenberg S, van Kleunen M. 2016. Evolutionary potential in the Alpine: trait heritabilities and performance variation of the dwarf willow Salix herbacea from different elevations and microhabitats. *Ecol Evol* **6**:3940–3952.

Shoeva (Tereshchenko) O, Khlestkina E, Gordeeva E, Arbuzova VS, Salina E. 2012. Relationship between anthocyanin biosynthesis and abiotic stress in wheat. *Proc15th EWAC Conf* **2011**:72–75.

Siepielski AM, Dibattista JD, Carlson SM. 2009. It's about time: The temporal dynamics of phenotypic selection in the wild. *Ecol Lett* **12**:1261–1276.

Snir A, Nadel D, Groman-Yaroslavski I, Melamed Y, Sternberg M, Bar-Yosef O, Weiss E. 2015. The Origin of Cultivation and Proto-Weeds, Long Before Neolithic Farming. *PLoS One* **10**:e0131422.

Stoffel MA, Johnston SE, Pilkington JG, Pemberton JM. 2021. Genetic architecture and lifetime dynamics of inbreeding depression in a wild mammal. *Nat Commun 2021 121* **12**:1–10.

Todesco M, Owens GL, Bercovich N, Légaré JS, Soudi S, Burge DO, Huang K, Ostevik KL, Drummond EBM, Imerovski I, Lande K, Pascual-Robles MA, Nanavati M, Jahani M, Cheung W, Staton SE, Muños S, Nielsen R, Donovan LA, Burke JM, Yeaman S, Rieseberg LH. 2020. Massive haplotypes underlie

ecotypic differentiation in sunflowers. *Nat 2020 5847822* **584**:602–607.

Urban MC. 2015. Accelerating extinction risk from climate change. *Science* **348**:571–573.

Volis S, Anikster Y, Olsvig-Whittaker L, Mendlinger S. 2004. The influence of space in genetic-environmental relationships when environmental heterogeneity and seed dispersal occur at similar scale. *Am Nat* **163**:312–327.

Volis S, Ormanbekova D, Shulgina I. 2016. Fine-scale spatial genetic structure in predominantly selfing plants with limited seed dispersal: A rule or exception? *Plant Divers* **38**:59–64.

Volis S, Ormanbekova D, Yermekbayev K, Song M, Shulgina I. 2015. Multi-Approaches Analysis Reveals Local Adaptation in the Emmer Wheat (Triticum dicoccoides) at Macro- but not Micro-Geographical Scale. *PLoS One* **10**:e0121153.

Wintle BA, Kujala H, Whitehead A, Cameron A, Veloz S, Kukkala A, Moilanen A, Gordon A, Lentini PE, Cadenhead NCR, Bekessy SA. 2019. Global synthesis of conservation studies reveals the importance of small habitat patches for biodiversity. *Proc Natl Acad Sci U S A* **116**:909–914.

Wright S. 1969. Evolution and the Genetics of Populations. Vol. 2: The Theory of Gene Frequencies. Chicago, University of Chicago Press.

Zeder MA. 2011. The origins of agriculture in the Near East. *Curr Anthropol* **52**.

Zheng X, Levine D, Shen J, Gogarten SM, Laurie C, Weir BS. 2012. A high-performance computing toolset for relatedness and principal component analysis of SNP data. *Bioinformatics* **28**:3326.

Zhu T, Wang L, Rodriguez JC, Deal KR, Avni R, Distelfeld A, McGuire PE, Dvorak J, Luo M-C. 2019. Improved Genome Sequence of Wild Emmer Wheat Zavitan with the Aid of Optical Maps. *G3 (Bethesda)* **9**:619–624.

Zsögön A, Peres LEP, Xiao Y, Yan J, Fernie AR. 2021. Enhancing crop diversity for food security in the face of climate uncertainty. *Plant J* **109**:402–414.

Supporting Information

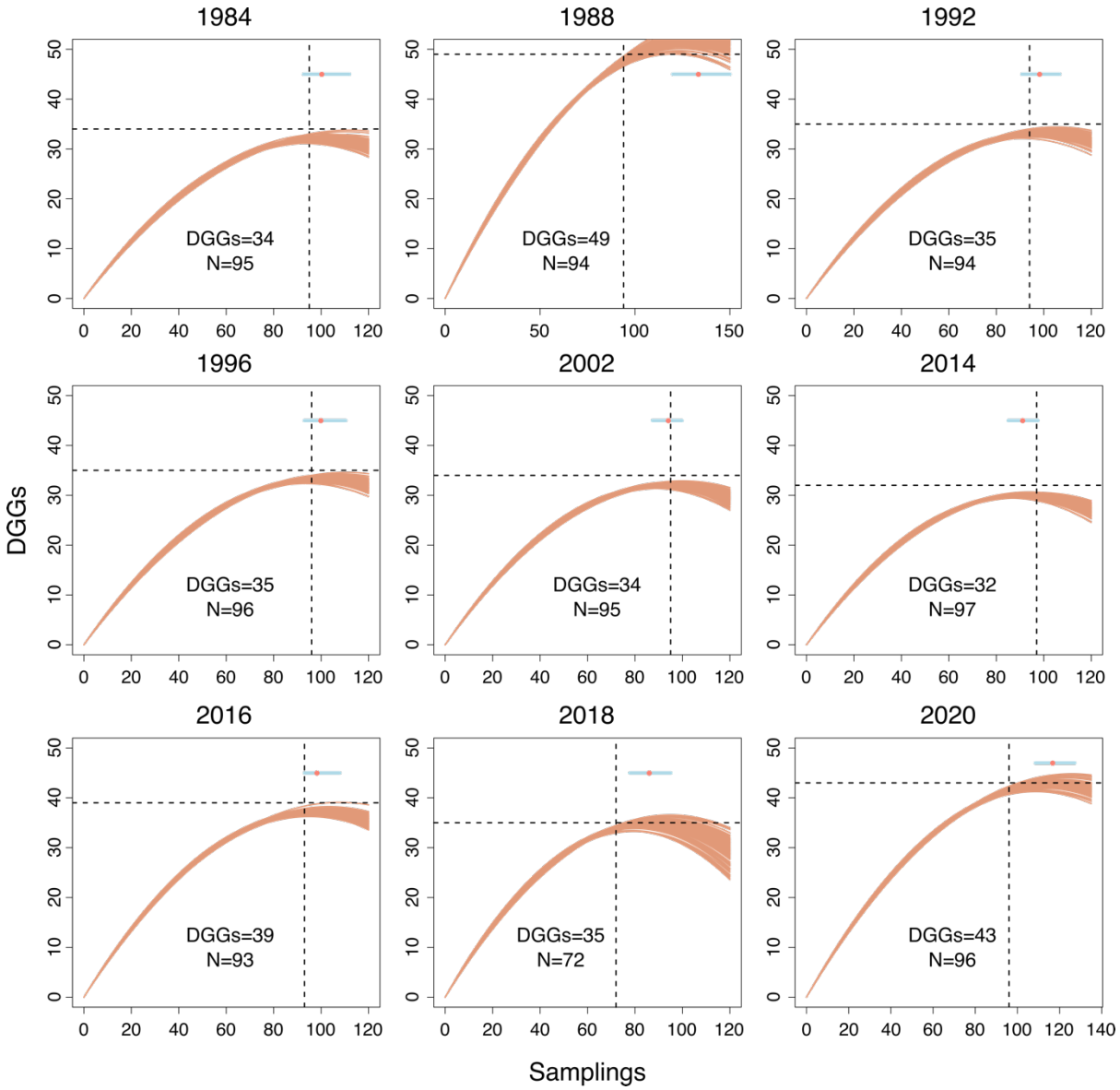

Figure S1. Rarefaction curves. Adjusted 2nd degree polynomials of 100x backwards sample of unique genotype number and number of samples collected per year. Dashed horizontal line represents the observed number of unique genotypes per year, dashed vertical lines represent number of samples per year. Light blue line and red dot represent range and mean of inflection points over replicate subsamples respectively.

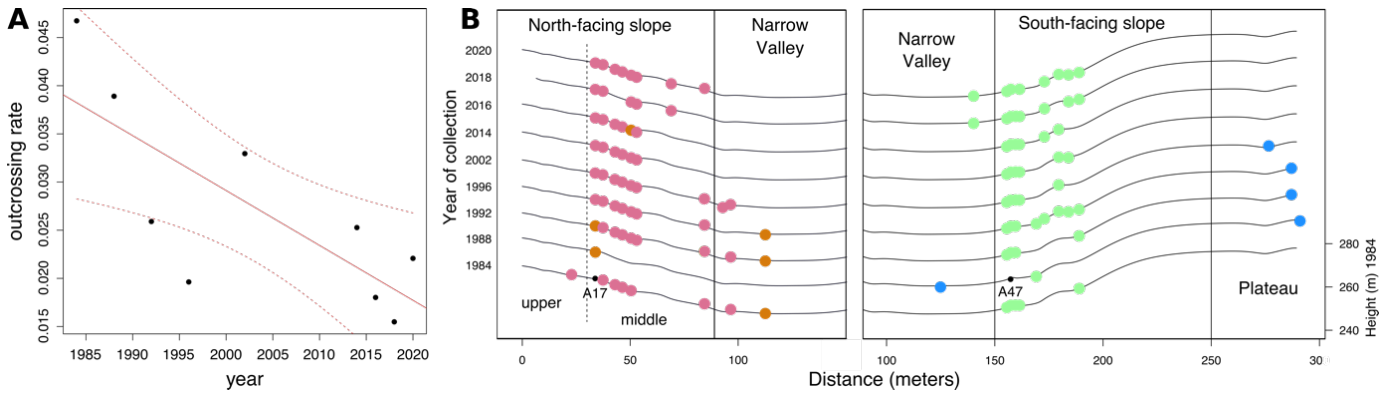

Figure S2. **Outcrossing in Ammiad.** (A) Outcrossing over time in Ammiad. The red continuous line represents the estimated average decrease of 0.06% every year, with confidence intervals shown as dashed lines. The highest rate of outcrossing is estimated for the middle north-facing slope, consistently with the identification of two highly heterozygous plants in this habitat from 1984 and 1988 (A17 and A20, respectively). Individual yearly estimates are shown as black dots. (B) Parental DGGs of 1984A17 (left panel) and 1988A47 (right panel) detected using SNPMatch. F1 plants are marked as a black dot.

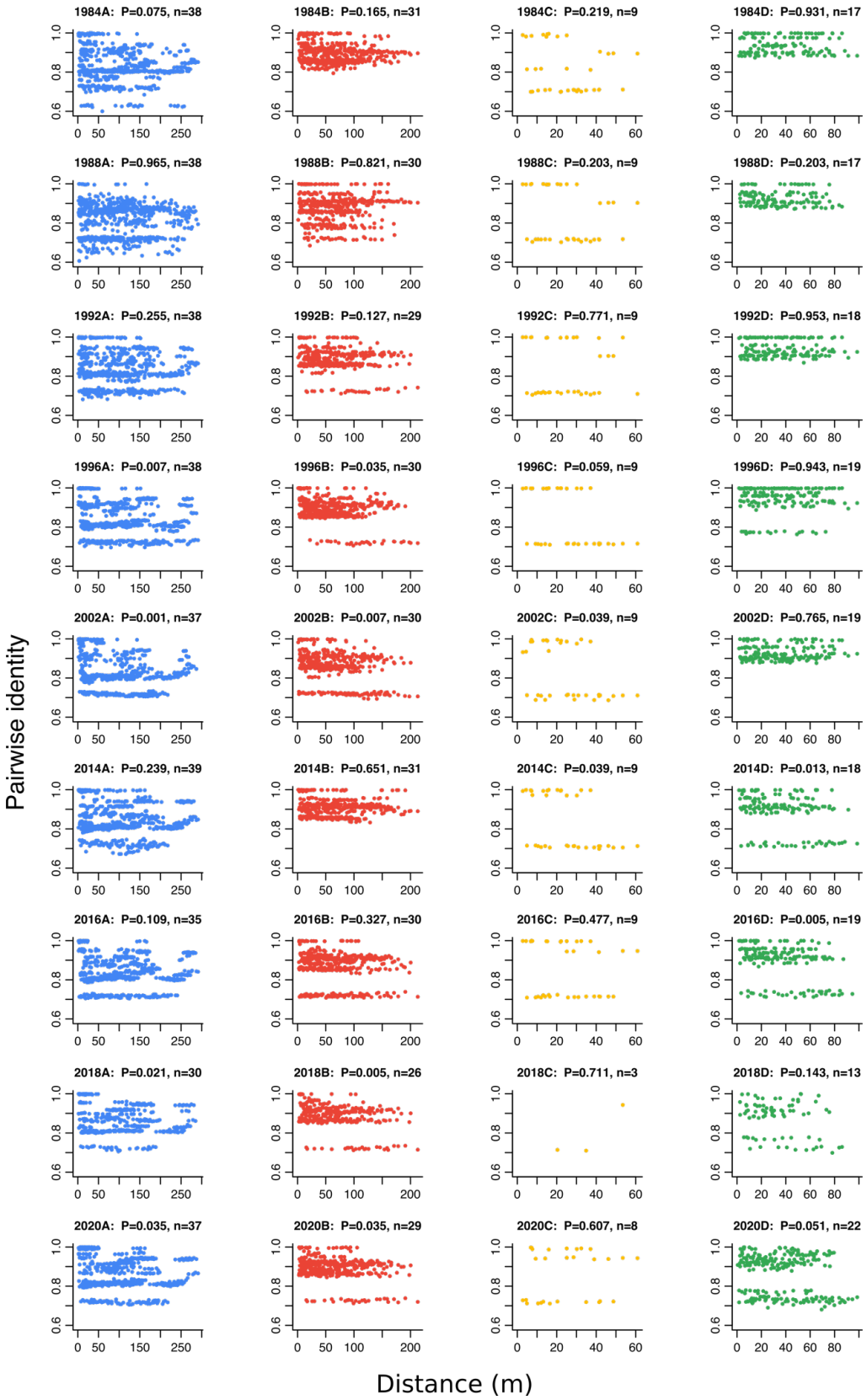

Figure S3. Correlation and significance of isolation by distance in Ammiad collection. Pairwise genetic identity by Euclidean distance (meters). Subplots show years of collection (rows) and transects (columns). The title of each plot indicates its number of samples and p-value from a Mantel test with 1000 permutations.

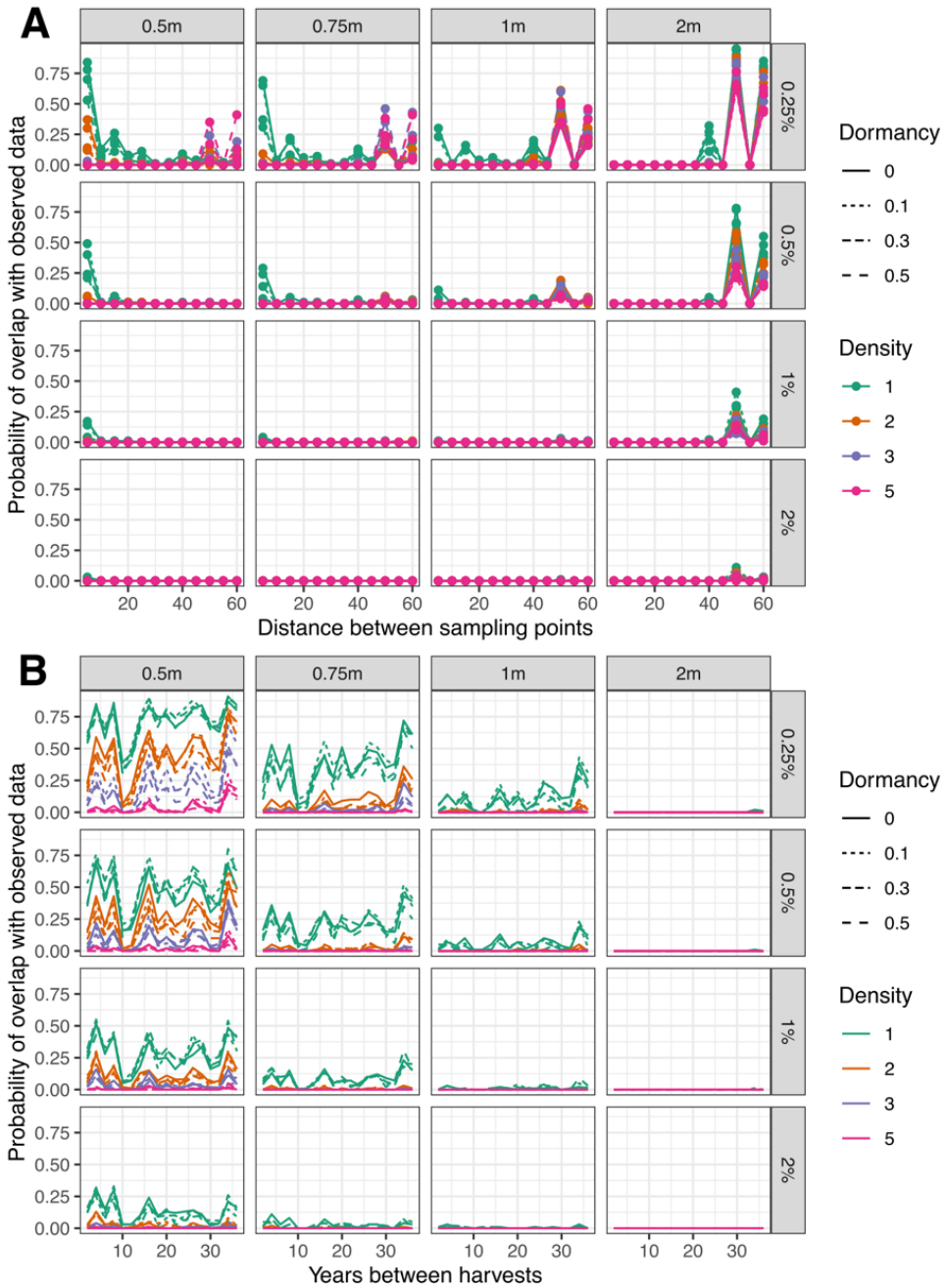

Figure S4. Overlap in spatial clustering between observed data and populations simulated under neutral demography and the probabilities that observed temporal stability could be generated by neutral demography. (A) The proportion of replicate simulations where pairs of sampling points at different distances were more likely to be occupied by plants of the same DGG than in any observed transect. **(B)** The proportion of replicate simulations where a single sampling point sampled in different harvest years was more likely to be occupied by plants of the same DGG than in any observed transect. Panels indicate increasing mean seed dispersal distances (left to right) and increasing outcrossing rates (top to bottom). 'Dormancy' indicates the proportion of seeds drawn from the seed bank in each generation, and 'Density' the number of plants per square meter.

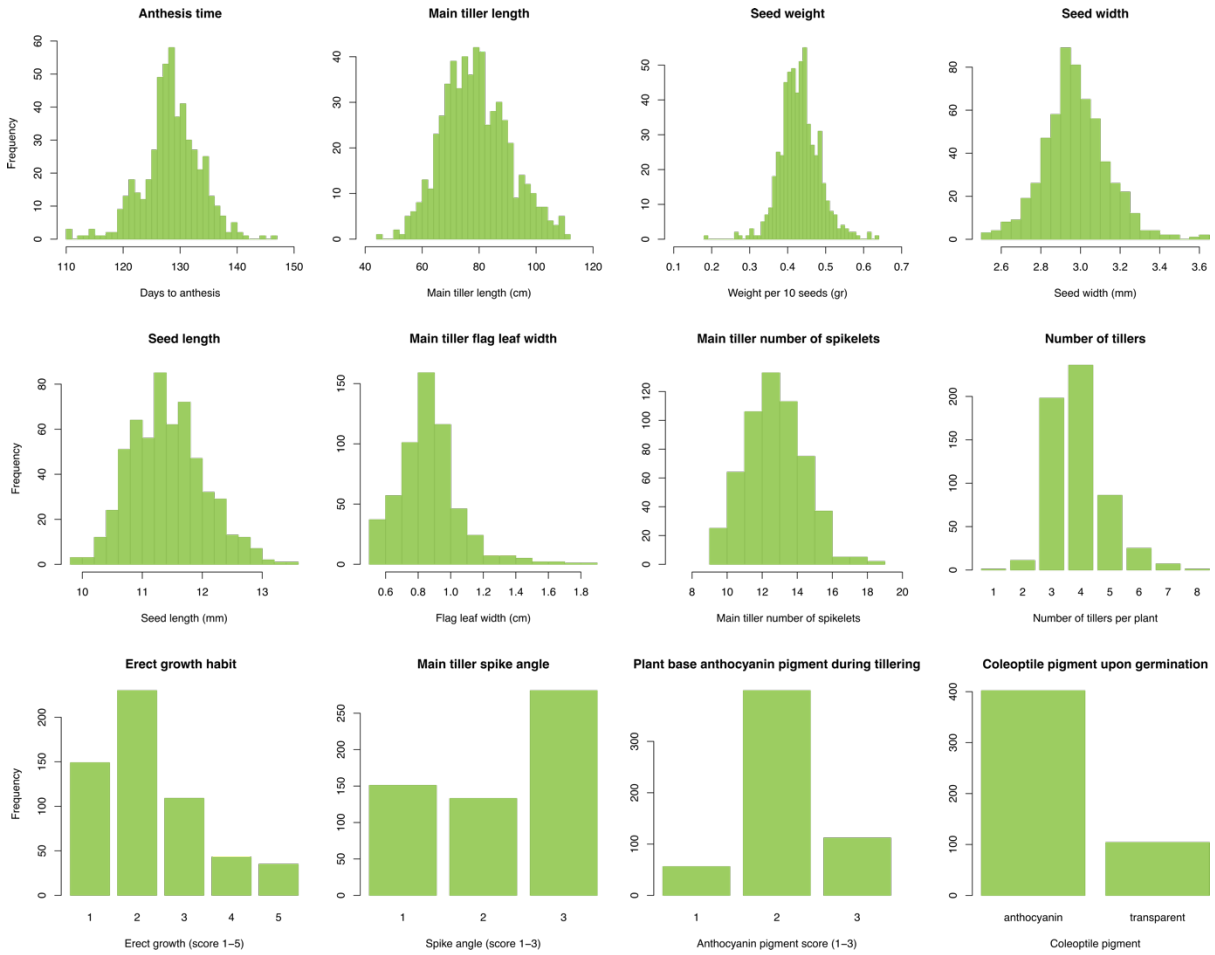

Figure S5. Distribution of phenotypes measured in common-garden experiment.

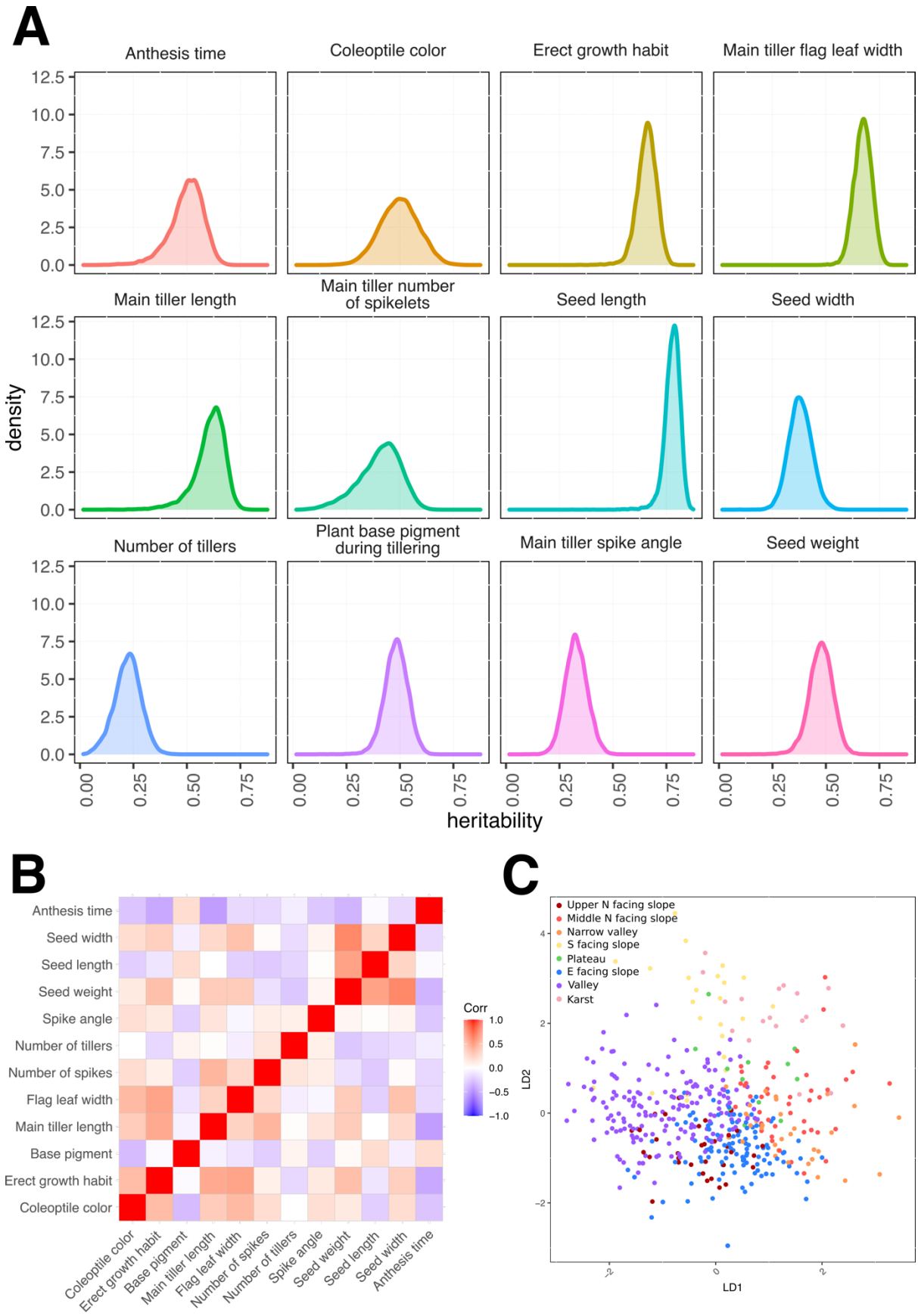

Figure S6. Trait heritability and phenotype-habitat linear discriminant analysis. (A) Posterior probability distribution of the heritability estimates across phenotypes. (B)

Correlation among phenotypes in the data used to estimate the role of habitat. Warmer colors indicate stronger positive correlation. (C) Projection of the first two dimensions of the linear discriminant analysis of the phenotypes of the genotypes sampled from the wild wheat Ammiad population. Different colors indicate genotypes distinctive of different habitats as defined in the text.

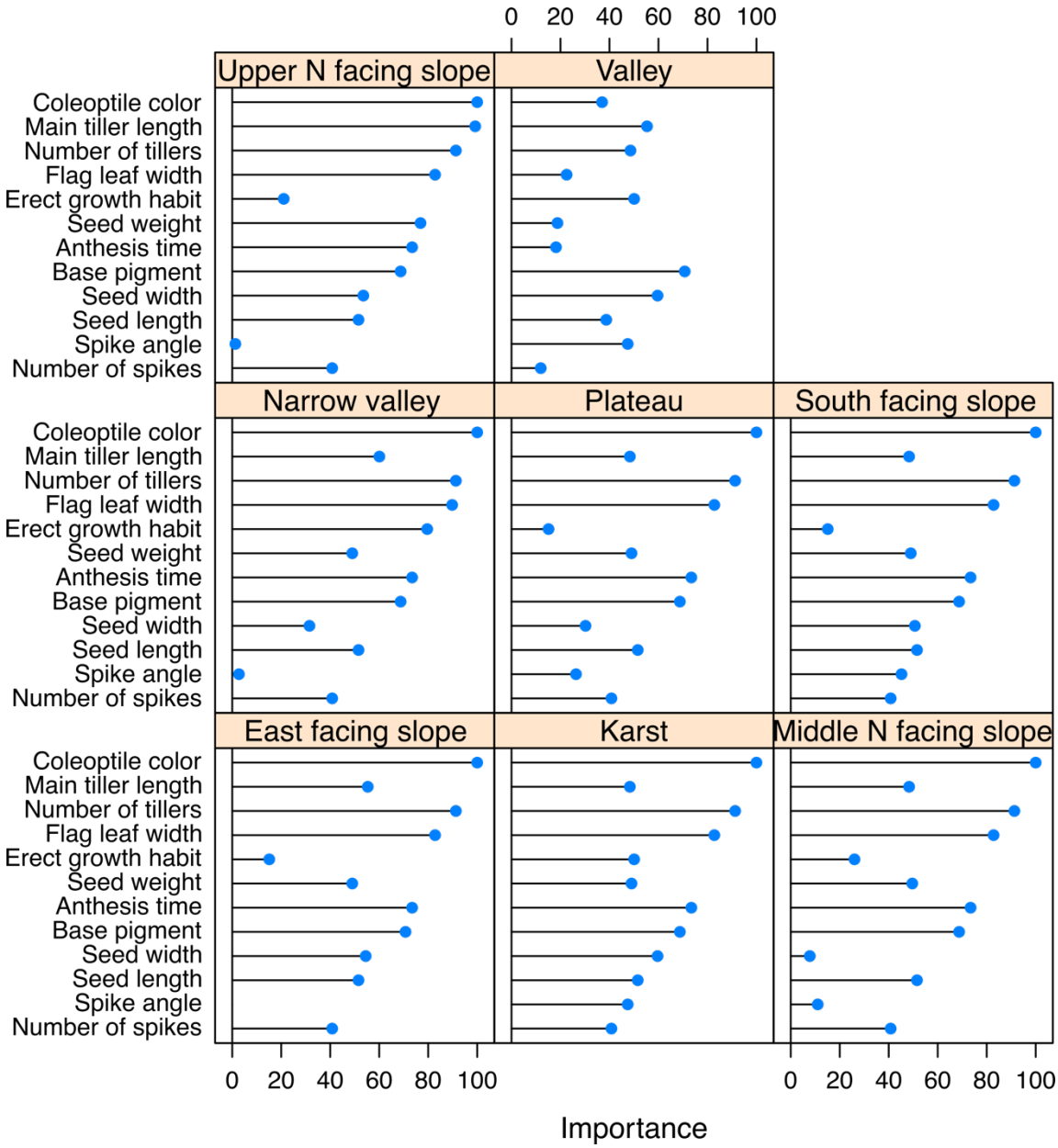

Figure S7. Phenotypes most relevant to distinguish different habitats according to the linear discriminant analysis, sorted top to bottom according to their overall importance across habitats.

Supplementary Tables

Table S1. Bootstrap-based ranges of F_{IS} and estimated outcrossing rates per habitat.

	F_{IS}	F_{IS}	outcrossing	outcrossing
Habitat	2.5%	97.5%	2.5%	97.5%
Upper North facing slope	0.9074	0.9246	0.0392	0.0485
Middle north facing slope	0.8385	0.8654	0.0722	0.0878
Narrow valley	0.9548	0.9627	0.0190	0.0231
South facing slope	0.9274	0.9348	0.0337	0.0377
Plateau	0.9565	0.9640	0.0183	0.0222
East facing slope	0.9294	0.9405	0.0307	0.0366
Valley	0.9535	0.9614	0.0197	0.0238
Karst	0.9082	0.9317	0.0354	0.0481

Table S2. Analysis of molecular variance of genotypes sampled in Ammiad across all years, subdivided by habitat, using only polymorphic sites within Ammiad. Sum of squared deviations (SSD) and mean square deviations (MSD), variance components (σ^2) and corresponding p-values were computed using the R package *pegas*. The Φ statistic for habitat was used as an estimate of the proportion of molecular variance explained by the habitat structure.

Component	**SSD**	**MSD**	**df**	**σ^2**	**p-value**	**Φ**
Habitat	0.9946	0.1421	7	0.0014	$<10^{-12}$	0.2833
Error	2.9429	0.0036	824	0.0036	/	/
Total	3.9374	0.0047	831	/	/	/

Table S3. Heritability of the phenotypes, measured as the proportion of variance among genotypes and blocks (growing plots) explained by genotype, using a Bayesian model implemented in the R package *brms* (Bürkner, 2017).

Phenotype	**heritability**	**Standard Deviation**
Seed length	0.78019	0.034308
Erect growth habit	0.663759	0.041745
Main tiller flag leaf width	0.657141	0.041966
Main tiller length	0.612437	0.073655

Plant base pigment during tillering	0.5053	0.05331
Coleoptile color	0.505163	0.090388
Anthesis time	0.500273	0.077041
Seed weight	0.485189	0.055428
Seed area	0.444486	0.052507
Main tiller number of spikelets	0.412969	0.097037
Seed width	0.384354	0.052098
Main tiller spike angle	0.358738	0.049909
Number of tillers	0.231275	0.062326
Germination date	0.029275	0.027938

Table S4. **Association between habitat and phenotypes.** Generalized linear mixed models comprising the random effect habitats were tested against a set of null models for each phenotype, not including habitat.

Phenotype	**p.value**	**Bonferroni corrected p.value**
Coleoptile color	0.001666	0.019988
Erect growth habit	0.092703	1
Plant base pigment during tillering	0.002859	0.034312
Main tiller length	0.249044	1
Main tiller flag leaf width	0.03783	0.453954
Main tiller number of spikelets	0.953601	1
Number of tillers	0.557119	1
Main tiller spike angle	0.34719	1
Seed weight	0.486148	1
Seed length	0.893096	1
Seed width	0.185839	1
Anthesis time	0.056984	0.683811

Table S5. Linear discriminant analysis dimension values.

	LD1	LD2	LD3	LD4	LD5
Coleoptile color	0.627	1.483	1.001	0.230	0.270
Erect growth habit	-0.330	0.115	0.093	-0.335	0.606

Plant base pigment during tillering	-0.651	0.036	0.508	-0.145	-0.114
Main tiller length	-0.288	0.128	-0.340	-0.332	-0.685
Main tiller flag leaf width	-0.384	0.373	-0.610	0.129	0.130
Main tiller number of spikelets	-0.055	-0.057	-0.175	0.315	0.157
Number of tillers	-0.233	-0.361	0.095	-0.320	0.010
Main tiller spike angle	0.304	-0.165	-0.094	-0.275	-0.462
Seed weight	0.015	0.219	-0.068	0.528	-0.965
Seed length	-0.533	-0.054	-0.126	0.017	0.413
Seed width	0.235	-0.549	-0.318	-0.819	0.518
Anthesis time	-0.249	-0.364	-0.620	0.339	-0.197

Movie S1 (separate file). Drone video of the different transects and microhabitats in Ammiad wild wheat reserve.

Dataset S1 (separate file). Dataset of Ammiad samples by genotype, coordinates and spike density measured at transect A in 2020.